

Design of A Heat Exchanger for Gas Turbine Inlet Air Cooling System

by

Abd Halim Bin Nurdin

Dissertation submitted in partial fulfillment of

the requirements for the

Final Year Project II

Bachelor of Engineering (Hons)

(Mechanical Engineering)

MAY 2011

Universiti Teknologi PETRONAS

Bandar Seri Iskandar

31750 Tronoh

Perak Darul Ridzuan

CERTIFICATION OF APPROVAL

Design of A Heat Exchanger for Gas Turbine Inlet Air Cooling System

by

Abd Halim Bin Nurdin

A project dissertation submitted to the
Mechanical Engineering Programme
Universiti Teknologi PETRONAS
in partial fulfilment of the requirement for the
BACHELOR OF ENGINEERING (Hons)
(MECHANICAL ENGINEERING)

Approved by,

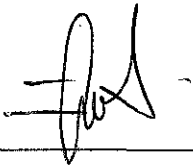


(Dr. Zainal Ambri B. Abd Karim)

UNIVERSITI TEKNOLOGI PETRONAS
TRONOH, PERAK
MAY 2011

CERTIFICATION OF ORIGINALITY

This is to certify that I am responsible for the work submitted in this project, that the original work is my own except as specified in the references and acknowledgements and that the original work contained herein have not been undertaken or done by unspecified sources or persons.



ABD HALIM BIN NURDIN

ABSTRACT

The ambient temperature has the greatest effect on gas turbine performance, due to change of the turbine air inlet-temperature and pressure ratio. Thus, thermodynamic analyses exposed that thermal efficiency and specific output decrease with an increase of humidity and ambient temperature. The aim of this project is to design a heat exchanger for gas turbine inlet air cooling system in order to increase the efficiency of the gas turbine. The project attempts to maintain a constant temperature of the inlet of gas turbine engine irrespective of the increasing in ambient temperature. This has been accomplished by developing a mathematical model based on the step by step techniques so that variation of all design parameters can be calculated. The author has set the tube diameter and number of rows as the variables while the other geometry parameters remain constant throughout this project. At the end, a set of variables data is compared to predict the heat exchanger performance. The increasing of the tube diameter and number of rows has increased the heat transfer coefficient and pressure drop in the system. Among the samples, the optimum design of the heat exchanger consisted of 26 rows of horizontal tube and 0.06185 m tube inner diameter.

ACKNOWLEDGEMENT

First of all, the author would like to express the utmost gratitude and appreciation to Allah because with His blessings, the Final Year Project (FYP) went very smoothly. Alhamdulillah, all praises to Him that the author are able to complete this project.

This project would not have been a successful task without the assistance and guidance of certain individuals and department whose contributions have helped in its completion. First and foremost, the author would like to thank to the project supervisor, Dr. Zainal Ambri B. Abd Karim for giving chance and full support in facilitate the author throughout the whole period of completing the FYP. His assistance and guidance from the beginning to the end of this project really help the author to complete the project successfully.

Special gratitude is also reserved for the Mechanical Engineering Department of Universiti Teknologi PETRONAS for providing excellent support in terms of providing new knowledge and information not just within the Final Year Project but also the five years spent while undergoing every lesson teach in pursuing mechanical engineering degree.

Finally many thanks to the author's family and fellow colleagues for their help and ideas throughout the completion of this study. I hope that the outcome of this report will bring beneficial output to others as well. Thank you very much everyone.

TABLE OF CONTENT

CERTIFICATION OF APROVAL.....	ii
CERTIFICATION OF ORIGINALITY.....	iii
ABSTRACT.....	iv
ACKNOWLEDGEMENT.....	v
TABLE OF CONTENT.....	vi
LIST OF FIGURES.....	ix
LIST OF TABLES.....	x
CHAPTER 1: INTRODUCTION.....	1
1.1 Background of Study.....	1
1.2 Problem Statement.....	2
1.3 Objectives	4
1.4 Scope of Study.....	5
CHAPTER 2: LITERATURE REVIEW.....	6
2.1 Effect of Ambient Temperature on Gas Turbine Performance.....	6
2.2 Selection Type of Heat Exchanger	8
2.3 Pressure Drop Correlations Over Tubes Banks.....	9
2.4 Heat Transfer Enhancement	9
CHAPTER 3: DESIGN METHODOLOGY.....	12
3.1 Tools.....	15
3.2 Progress	15

CHAPTER 4: MATHEMATICAL MODEL.....	16
4.1 Thermal Properties.....	16
4.2 Mass Flow Rate.....	16
4.3 Log Mean Temperature Difference.....	17
4.4 Sizing Constraint.....	18
4.5 Physical Characteristics of Fin Tube Heat Exchanger.....	19
4.6 Air Side.....	21
4.6.1 Reynolds Number.....	21
4.6.2 Convective Air Heat Transfer Coefficient.....	23
4.6.3 Pressure Loss.....	23
4.7 Water Side.....	25
4.7.1 Reynolds Number.....	25
4.7.2 Convective Water Heat Transfer Coefficient.....	25
4.7.3 Pressure Loss.....	26
4.8 Overall Heat Transfer Coefficient.....	29
4.9 Fin Efficiency for Radial Fin.....	29
4.10 Heat Transfer Area.....	32
CHAPTER 5: RESULTS AND DISCUSSION.....	34
5.1 General.....	34
5.2 The Effect of Ambient Temperature on the Chilled Water Mass Flow Rate.....	34

5.3 Analytical Model Results for Heat Exchanger Design.....	36
5.3.1 Effect of Number of Row to the Total Heat	
Transfer Rate for Air Side.....	36
5.3.2 Effect of Tube Diameter to the Heat Transfer	
Coefficient.....	37
5.3.3 Effect of Number of Rows to the Pressure Drop.....	38
5.3.4 The Air Outlet Temperature.....	39
5.4 Final Core Design.....	41
CHAPTER 6: CONCLUSION.....	43
CHAPTER 7: RECOMMENDATIONS.....	44
REFERENCES.....	45
APPENDIX A: THERMAL PROPERTIES OF SATURATED	
LIQUID WATER (H₂O).....	46
APPENDIX B: THERMAL PROPERTIES OF GASES AT	
ATMOSPHERIC PRESSURE.....	47
APPENDIX C: THERMAL PROPERTIES OF METALLIC SOLIDS.....	48
APPENDIX D: PIPE DIMENSIONS.....	48
APPENDIX F: HEAT EXCHANGER PERFORMANCE	
SPREADSHEET.....	49
APPENDIX G: THE OVERALL PERFORMANCE OF	
HEAT EXCHANGER SPREADSHEET.....	51

LIST OF FIGURES

Figure 1.1	An overview of the GDC process plant layout	1
Figure 1.2	Air cooled heat exchanger from chilled water system	2
Figure 1.3	An overview of the problem statement	3
Figure 2.1	Variation of power output with ambient temperature	6
Figure 2.2	Variation of the heat rate with ambient temperature	7
Figure 2.3	The arrangement of tube bank. (a) Inline and (b) staggered Arrangement	8
Figure 2.4	Radial fin geometry	10
Figure 2.5	Radial fin efficiency	11
Figure 3.1	Flow chart of the methodology used in the research	14
Figure 4.1	(a) Chilled water coil construction	20
	(b) A 4-row coil with a 4-tube face	20
	(c) Geometry of the radial fin perpendicular to tube	20
	(d) Tube transverse and longitudinal pitch in tube bank	20
Figure 4.2	The friction factor for staggered tube bank is a function of the Reynolds number	24
Figure 5.1	Ambient air temperature versus mass flow rate	35
Figure 5.2	Ambient air temperature versus heat transfer rate	35
Figure 5.3	Total heat transfer rate versus number of rows	36
Figure 5.4	Heat transfer coefficient versus tube diameter for air side	37
Figure 5.5	Heat transfer coefficient versus tube diameter for water side	38
Figure 5.6	Pressure drop versus number of rows for air side	39
Figure 5.7	Pressure drop vs number of rows for water side	39
Figure 5.8	Air outlet temperature comparison for the samples based on the Number of row in the tube bank	40
Figure 5.9	General configuration of fin tube heat exchanger	42

LIST OF TABLE

Table 1.1	Operating and nominal parameter of GTE	4
Table 2.1	Influence of the relative humidity on the thermal load	7
Table 3.1	Outer and inner tube diameter for each sample	13
Table 3.2	Number of rows for each sample	13
Table 3.3	List of activities during the project	15
Table 4.1	Thermal properties of the hot air and chilled water	16
Table 4.2	Typical overall heat transfer coefficients	19
Table 4.3	The heat exchanger geometrical data	21
Table 4.4	Roughness for new pipe and ducts is a function of material and manufacturer	27
Table 5.1	Final design of the fin tube heat exchanger	41

CHAPTER 1 INTRODUCTION

1.1 Background of Study

Gas District Cooling (GDC) plant in Universiti Teknologi PETRONAS is a cogeneration plant which produces both electrical power and chilled water for space cooling in UTP. Since then, the electrical power and chilled water are continuously supplied to UTP. Cogeneration is a form of energy conservation process, because of the heat energy recovery that can be lost from the gas turbine exhaust. It consist of gas turbine engine (GTE), heat recovery steam generator (HRSG), steam absorption chiller (SAC), air cooled chiller (ACC), cooling tower (CT), and thermal energy storage (TES). The gas turbine engine drives the electric generator for production of electrical power. The exhaust heat from the gas turbine is utilized for steam production which is needed for heating in the steam absorption chiller. The chilled water produced from the steam absorption chiller is used for air conditioning of the building in UTP. The whole GDC plant is shown in **FIGURE 1.1**.

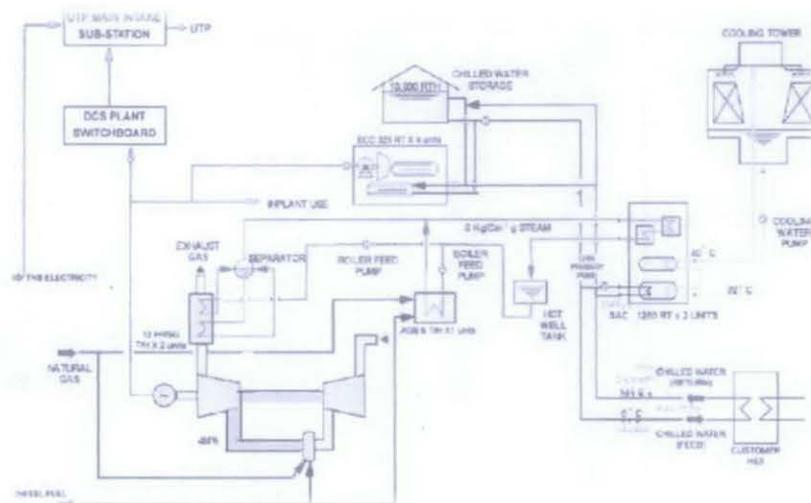


FIGURE 1.1: An overview of the GDC process plant layout (*taken from GDC operational manual*)

The three main parameters that affect the performance of a gas turbine are the intake air temperature, intake air pressure, and the air-inlet and exhaust-gas head losses. Thermodynamic analyses exposed that thermal efficiency and specific output decrease with an increase of humidity and ambient temperature. Therefore, this project proposed to add an air cooler unit at the air inlet intake of the gas turbine in order to reduce the ambient temperature, thus, the efficiency of the gas turbine will be increase.

1.2 Problem Statement

Gas turbine operates in an ambient condition that is constantly changing which affects the performance and efficiency of the plant. It is known that the efficiency of the gas turbine is relatively low at design point and it worsens further at part load and at off design at high ambient temperatures especially during the hot days. One way to address this is by placing an air cooler which is a heat exchanger at the intake side of the gas turbine which could maintain a constant air inlet temperature into the gas turbine as shown in **FIGURE 1.2**. The design of the heat exchanger must take into account the air volume flow, pressure drop, cooling capacity and demand variation. In addition, the cooling effectiveness, capacity and efficiency of the heat exchanger are analyzed in order to get an optimum design.

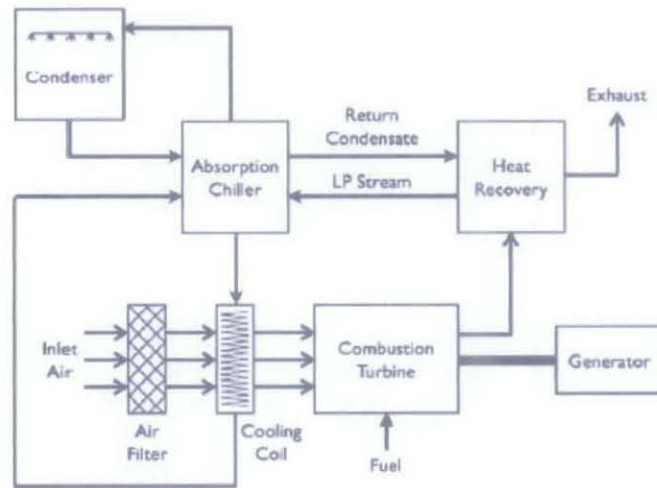


FIGURE 1.2: Air cooled heat exchanger from chilled water system (Amell and Cadavid (2002)).

This project required to design a fin tube air cooler unit installed at the air inlet intake of gas turbine. The refrigerant or chilled water at $6\text{ }^{\circ}\text{C}$ enters the first row and leaves the coil from the last row at $13\text{ }^{\circ}\text{C}$. The hot air from ambient then to be cooled from $36\text{ }^{\circ}\text{C}$ to $20\text{ }^{\circ}\text{C}$ as passing cross the tubes prior entering the compressor. The mass flow rate of the air had to be 19 kg/s same with the nominal value at inlet intake for the compressor in the gas turbine engine. The theoretical model to predict the performance of this heat exchanger is generated based upon working parameters of the plant.

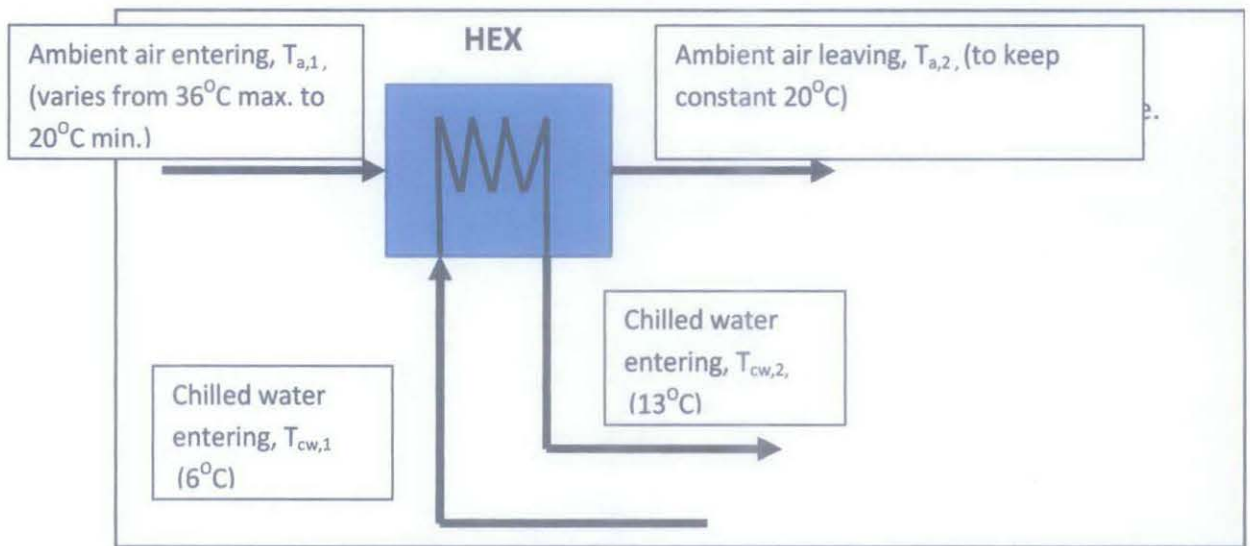


FIGURE 1.3: An overview of the problem statement

TABLE 1.1: Operating and nominal parameter of GTE. (*taken from GDC operation daily report*)

Component	Parameters	Nominal value	Operating range
Air Compressor	Mass flow rate, m_a	19 kg/s	14-19 kg/s
	Temperature, T_a	<32 °C	27 – 35 °C
	Compression ratio, r_c	11.7	
Combustion Chamber	Mass flow rate, m_f	0.26 kg/s	0.26 – 0.3 kg/s
	Low heating value, LHV	41000 kJ/kg K	
Turbine	Temperature, T_g	923 K	903 – 923 K
	Net work, W_{net}	4.2 MW	2.44 – 3.26 MW
	Turbine Exhaust Temperature, TET	450 °C	446 – 450 °C

1.3 Objectives

The objectives of this project are:

- i. To design a fin tube type heat exchanger for gas turbine inlet air
- ii. To analyze the cooling effectiveness, capacity and efficiency of the heat exchanger

1.4 Scope of Study

This project is aim to design of a coil type heat exchanger that can be fix into a gas turbine air inlet at the GDC plant in UTP. During the process, research and study has to be made to find the best design for the heat exchanger and able to utilize and demonstrate the principles of thermodynamics and heat transfer in solving this matter. During the design phase, the author has used Computer Aided (CAD) software like CATIA in designing the structure in developing 2D and 3D modeling of the structure.

The study on the 2D and 3D modeling is to predict the parameters and analyze the structure of the design. This involves the study on the characteristic flow of the fluid under certain parameters and to calculate the efficiency of the heat exchanger. The process has completed within approximately one year timeframe (two semesters).

CHAPTER 2

LITERATURE REVIEW

2.1 Effect of Ambient Temperature on Gas Turbine Performance

Amell and Cadavid (2002), study the effect of ambient temperature on the gas turbine performance and the influence of the relative humidity on the air cooling thermal load in gas turbine power plant. It is said that in heavy turbines, the increasing in the ambient temperature does not significantly affect the volumetric flow, but it does affect the air mass flow, due to the density reduction.

Since the net power output is directly proportional to the air mass flow, it decreases when ambient temperature increases. As the result, from **FIGURE 2.1** and **FIGURE 2.2** show the power output and heat rate variations on relation to the ambient temperature for a gas turbine that at ISO conditions has a power output of 160 MW.

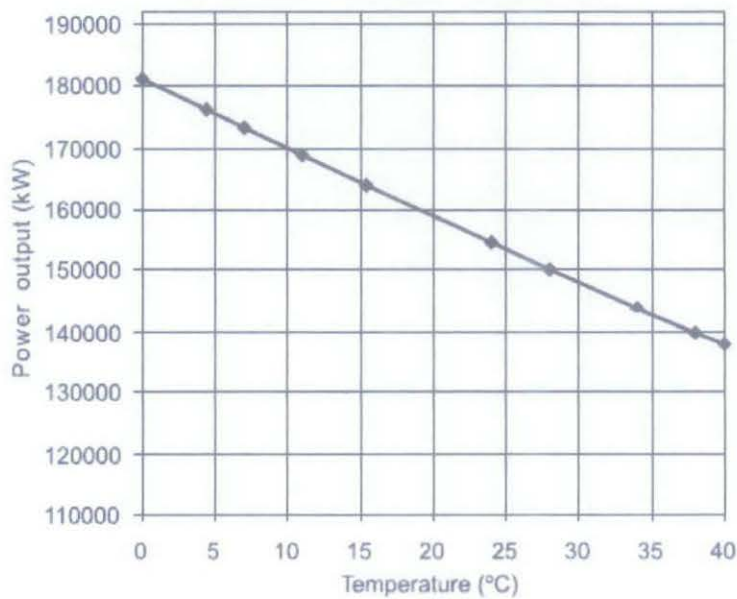


FIGURE 2.1: Variation of power output with ambient temperature (Amell and Cadavid (2002)).

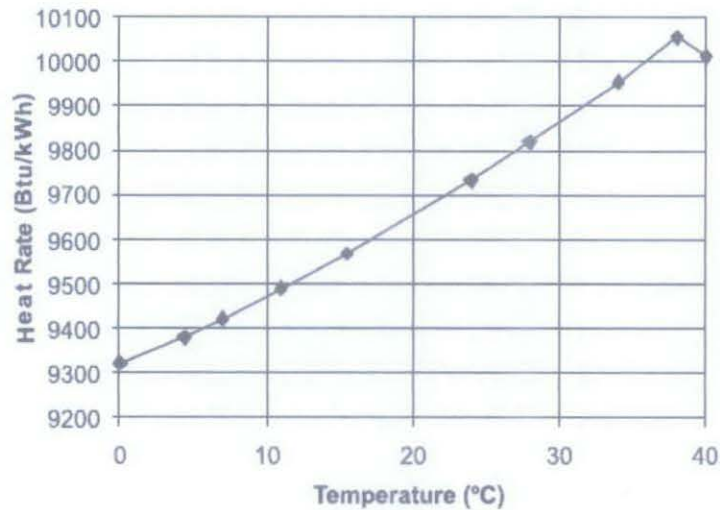


FIGURE 2.2: Variation of the heat rate with ambient temperature (Amell and Cadavid (2002)).

They described that the thermal load depends on the air mass flow, on the relative humidity, on the ambient temperature and on the cooling temperature. Thus the increase in the relative humidity has a great influence in the thermal load values. In determination of the influence of the relative humidity on the thermal load for gas turbines, the analysis had been carried out using a 160 MW turbine that the air mass flow is cooled up to 4.4 °C. The evaluation is carried out considering three relative humidity values, which are 34%, 60% and 80% respectively. From the result (TABLE 2.1), it is noticed that the higher the relative humidity, the more the air-cooling thermal load that enters the turbine.

TABLE 2.1: Influence of the relative humidity on the thermal load

Relative humidity (%)	Thermal load (ton)	Ratio
34	8.620	1.00
60	13.183	1.53
80	16.765	1.94

2.2 Selection Type of Heat Exchanger

Khan, et al. (2006), had study on the heat transfer on the variation of pitch ratio for both in-line and staggered tube bundles. They develop analytical models for heat transfer from in line and staggered tubes banks as in **FIGURE 2.3** respectively and compared their predicted results with the present analysis for compact and widely spaced bank. These models are developed depending on the longitudinal and transverse pitches, Reynolds and Prandtl numbers. In developing these models, it is assumed that the flow is steady, laminar, fully developed.

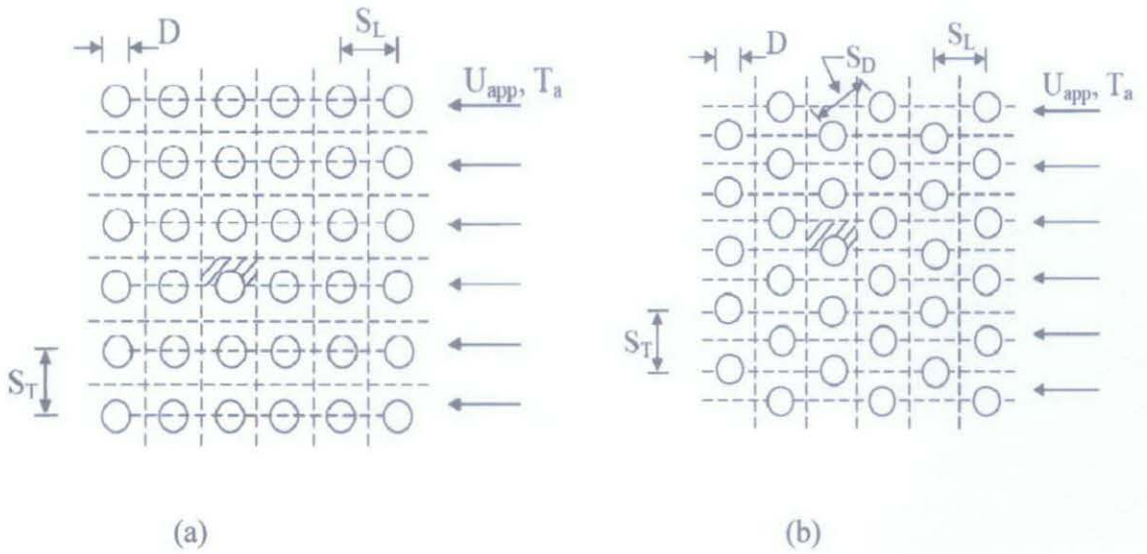


FIGURE 2.3: The arrangement of tube bank. (a) Inline and (b) staggered arrangement

As the conclusion, for both arrangements, the heat transfer increases mostly with decreasing longitudinal pitch ratio, and vice versa. From the comparison, it is observed that compact banks (in line or staggered banks) indicate higher heat transfer rates than widely spaced ones. Also for the constant pitch ratio, the heat transfer is higher in a staggered bank than in an in-line bank. Thus, it is clear that staggered tubes bank had a higher heat transfer rate.

Compact Heat Exchanger

Compact heat exchangers have been widely used in various applications in thermal fluid systems including automotive thermal management systems. Radiators for engine cooling systems, evaporators and condensers for HVAC systems, oil coolers, and intercoolers are typical examples of the compact heat exchangers which can be found in ground vehicles. Among the different types of heat exchangers for engine cooling applications, cross flow compact heat exchangers with circular fins are of a special interest. This is because of their higher heat performance capability with the lower flow resistance.

2.3 Pressure Drop Correlations over Tubes Banks

Genic, et al. (2005), had done a research on air pressure drop in helically-finned tube heat exchangers. Thus, they proposed new correlations for estimation of air pressure drop in helically-finned tube bundles with in-line and staggered tube arrangement. First, they develop a mathematical model of heat exchanger, which geometrical parameters are taken from open literature (Kays and London, and Yudin) to make a correlations analyze pressure drop of the helically finned heat exchanger for both densely packed staggered tube and inline bundles. From these correlations, they can be used in design of helically finned tube heat exchanger in varying Reynolds numbers and geometrical parameters in order to measure the pressure drop through the heat exchanger.

2.4 Heat transfer enhancement

To analyze the exchanger heat transfer problem, a set of assumptions are introduced so that the resulting theoretical models are simple enough for the analysis. The following assumptions and idealizations are made for the exchanger heat transfer problem formulations.

1. The heat exchanger operates under steady-state conditions (constant flow rates and fluid temperature).
2. Heat losses to or from the surrounding are negligible (adiabatic process).

3. No energy sources or sinks in the exchanger walls or fluids
4. The temperature of each fluid is uniform over every cross section.
5. Wall thermal resistance is distributed uniformly in the entire heat exchanger.
6. The individual and overall heat transfer coefficient is constant throughout the system.
7. The specific heat of each fluid is constant.

Ramesh and Sekulic, (2003), explained that, in order to increase the heat transfer area, extended surface can be attached to the primary surface of the tubes. Such as fins. Thus, heat is conducted through the fin to the surrounding fluid, or vice versa by convective heat transfer method. As a result, the addition of fins to the primary surface reduces the thermal resistance on that side and thereby increases the total heat transfer from the surface for the same temperature difference. Yet, for some cases, the addition of the secondary surfaces will cause decreasing in pressure drop.

Fin Efficiency for Radial Fin

For radial fin the geometry as illustrated in **FIGURE 2.4**, the inside and outside radius are R_i and R_o respectively, and the fin has a uniform thickness t . the outside edge of the fin at $r= R_o$ is defined as the fin tip. The origin is located at the center of the cylinder at $r=0$ even though the fin itself begins at $r=R_i$.



FIGURE 2.4: Radial fin geometry (Shah and Sekulic, 2003)

The solution of the equation subject to the preceding boundary conditions involves Bessel functions, special functions with problems with circular or cylindrical symmetry. The author presents the efficiency of a radial fin in graphical form in **FIGURE 2.5**.

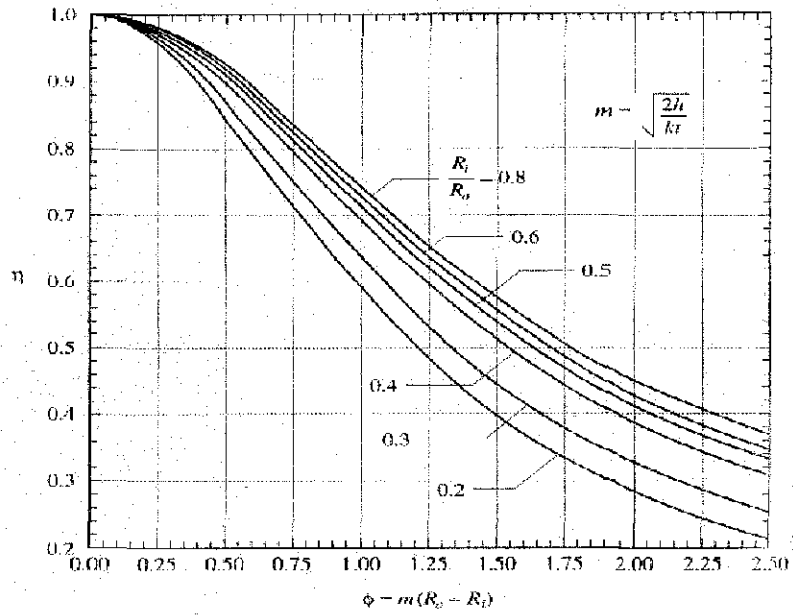


FIGURE 2.5: Radial fin efficiency (Shah and Sekulic, 2003)

CHAPTER 3

DESIGN METHODOLOGY

An overview of the methodology of heat exchanger design is presented in this section. The methodology of this research is presented in **FIGURE 3.1**. The research starts with the background study of the gas turbine intake requirement and the effect of ambient conditions (temperature, relative humidity and pressure). The study then proceeds with understanding the principles of heat transfer between circulating chilled water and air through coils, plates or tubes. At this stage, the author had to identify what are the laws or principles that are associated with the heat exchanger design. These include fluid mass flow rates, fluids types and its properties, temperatures and pressures at both inlets, fouling effect, pressure drop and also heat transfer rate.

After that, the research proceeds to the next stage which is to study of heat exchanger design parameters and standards. A proper selection of the material and type of heat exchanger whether it is plate or fin-tube is made depending on the operating temperature, pressures, type of fluids used, heat flow rate and its thermal resistance according to international standards (such as ASME or TEMA standards).

Next stage is to develop a heat exchanger with high air flow rate, large temperature reduction range, and minimal pressure drop across the cooler. During this stage, an estimation of heat exchanger core parameters is introduced taking into consideration of the area of the turbine inlet, desired heat transfer rate and outlets temperature to develop a mathematical model. This model is used as the platform for the author to make the analysis for the heat exchanger performance. For comparison analysis, the author has introduced six sample of data in which has different tube diameters and different number of tubes as the variables as shown in **TABLE 3.1** and **TABLE 3.2**. The others parameters such as fin geometry, frontal area are assumed to be fix throughout the analysis. This variables however has been made based on the standard from the reliable resources, for instance, the tube diameter can be found from the **APPENDIX D**

TABLE 3.1: Outer and inner tube diameter for each sample.

	Tube Outer Diameter, D_o (m)	Tube Inner Diameter, D_i (m)
Sample 1	0.02858	0.02527
Sample 2	0.03493	0.03162
Sample 3	0.04128	0.03762
Sample 4	0.05398	0.04976
Sample 5	0.06668	0.06185
Sample 6	0.1302	0.122

TABLE 3.2: Number of rows for each sample.

	Number of Rows				
Sample 1	18	20	22	24	26
Sample 2	18	20	22	24	26
Sample 3	18	20	22	24	26
Sample 4	18	20	22	24	26
Sample 5	18	20	22	24	26
Sample 6	18	20	22	24	26

*each row has a fixed number of 20 tubes.

In the end, a set of data comprising all the heat exchanger is summarized for the comparison analysis at the same time has been used to find the optimum heat exchanger design and the desired temperature outlet.

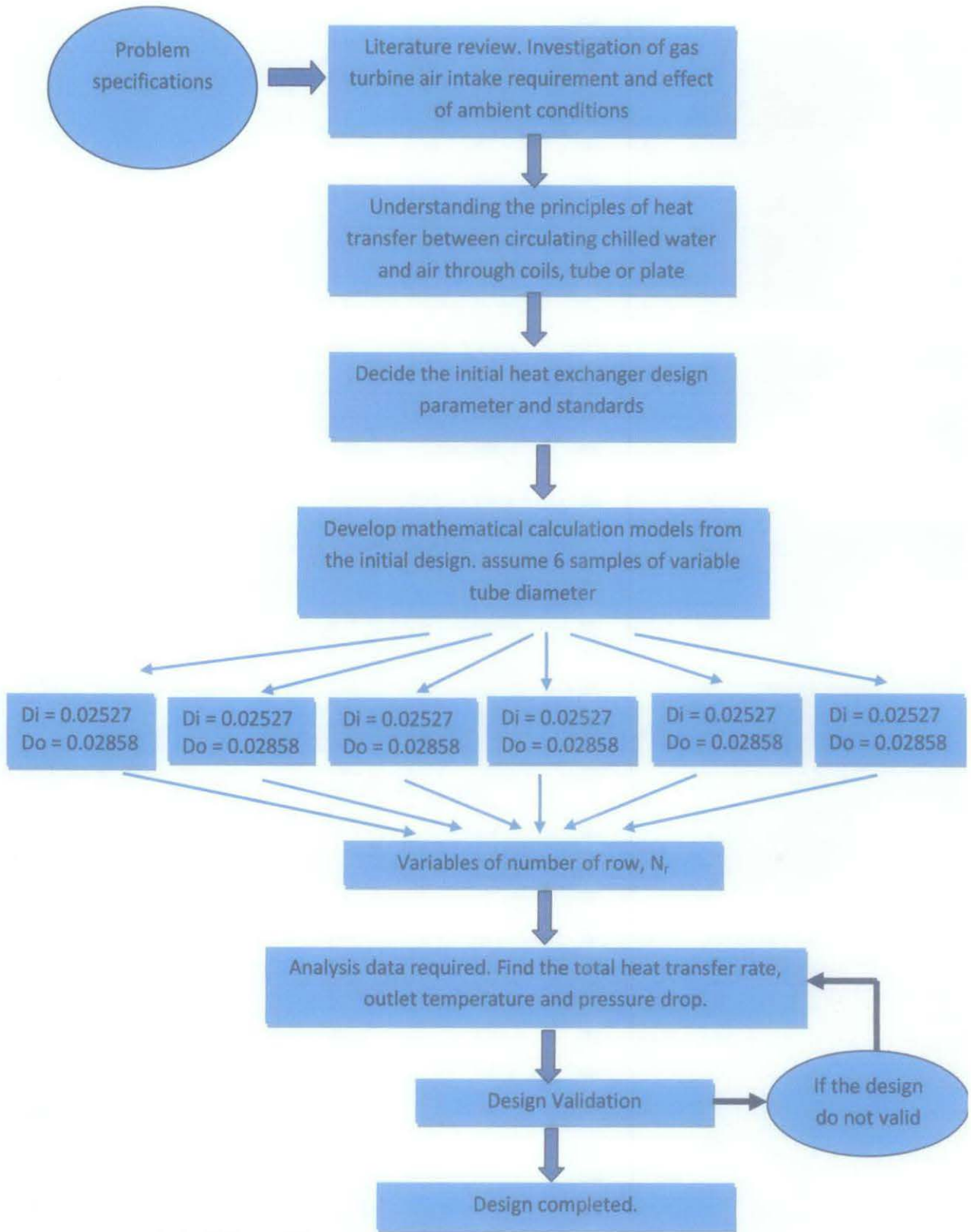


FIGURE 3.1: Flow chart of the Methodology used in the research

3.1 Tools

3.2.1 CATIA

The software used to develop the 3D modeling of the structure and analyze of the structure.

3.2.2 Microsoft Excel

Used to generate data from the variables geometry data for further analysis

3.2.3 Online Resources and Journals

Literature review study and reference for standards

3.2 Progress

a) Gantt chart

TABLE 3.3: List of Activities during the project

No	Details work	1	2	3	4	5	6	7	Mid-semester Break							
		8	9	10	11	12	13	14								
1	Project Work Continues															
	a) continuity from FYP 1 (Heat Exchanger Thermal Design)															
	b) compute heat transfer coefficient & overall efficiency															
	c) Numerical Modeling of Cross Flow Compact Heat Exchanger (FLUENT)															
2	Submission of Progress Report															
3	Project Work Continues															
	a) Modeling design and meshing															
	b) Computational Model Results for Heat Exchanger															
4	Pre-EDX															
5	Submission of Draft Report															
6	Submission of Dissertation (soft bound)															
7	Submission of Technical Paper															
8	Oral Presentation															
9	Submission of Project Dissertation (hard bound)															

CHAPTER 4

MATHEMATICAL MODEL

4.1 Thermal Properties

The first step in making the calculations is to find all the values of thermal properties in regard of designing the heat exchanger. Both air and water properties are based on the inlet temperatures which are 36 °C for air and 6 °C for water respectively (APPENDIX A and B). The thermal properties of liquid are given in the TABLE 4.1 below.

TABLE 4.1: Thermal properties of the hot air and chilled water

Properties	Outside tubes: Hot air	Inside tubes: Chilled water
Inlet temperature, T_{in} (°C)	36	6
Outlet temperature, T_{out} (°C)	20	13
Heat capacity, C_p (kJ/kg.K)	1.007	4.183
Thermal conductivity, k (W/m.K)	0.0263	0.579
Dynamic Viscosity, μ (kg/m.s)	184.6×10^{-7}	14805.2×10^{-7}
Kinematic Viscosity, ν (m ² /s)	15.89×10^{-6}	148.06×10^{-8}
Density, ρ (kg/m ³)	1.1614	1000
Prandtl number, Pr	0.707	10.69

4.2 Mass Flow Rate

To compute heat transfer rate for ambient air, first need to find convective heat transfer rate using Newton's law of cooling

$$\dot{Q}_h = (\dot{m}_1 c_p) \Delta T$$

$$\begin{aligned}\dot{Q}_h &= \left(\frac{19 \text{ kg}}{\text{s}}\right) \left(\frac{1.007 \text{ kJ}}{\text{kg.K}}\right) (309 - 293)\text{K} \\ &= 306.128 \text{ kW}\end{aligned}$$

From the theory of energy balance equation, heat transfer out from hot air is equal to the heat transfer in chilled water. Thus the mass flow rate for chilled water is;

$$\begin{aligned}\dot{Q}_h &= \dot{Q}_c = C_c \Delta T \\ 306.128 \text{ kW} &= \dot{m}_2 \left(\frac{4.198 \text{ kJ}}{\text{kg.K}}\right) (286 - 279)\text{K} \\ \dot{m}_2 &= 10.42 \text{ kg/s}\end{aligned}$$

Hence, to have the desired temperature difference, it is required to transfer 306.128 kW of heat from the air by the chilled water and the required mass flow rate for chilled water is 10.42 kg/s.

4.3 Log Mean Temperature Difference

Temperature of fluids varies along the heat exchanger, thus to overcome this difference, we used the LMTD method to have the average temperature differences in each fluids. For log mean temperature difference (LMTD) is given by this equation; where the subscripts *a* and *w* refer to the air and water respectively.

$$\begin{aligned}\Delta T_{lm} &= \left[\frac{(T_{a,in} - T_{w,out}) - (T_{a,out} - T_{w,in})}{\ln \left[\frac{(T_{a,in} - T_{w,out})}{(T_{a,out} - T_{w,in})} \right]} \right] \\ &= \left[\frac{(309 - 286) - (293 - 279)}{\ln \left[\frac{(309 - 286)}{(293 - 279)} \right]} \right] \\ &= 18.13^\circ\text{C} = 18.13 \text{ K}\end{aligned}$$

4.4 Sizing Constraint

One of the good approaches to the sizing problem was to make a rough estimation of the values for the physical core characteristic of the fin tube heat exchanger in the region of the interest and then using the analytical approaches to come out with a design calculation model. Then we calculated the performance for comparison with the specified performance, (Shah and Sekulic, (2003)). In developing these models, it is assumed that the flow is steady, laminar, and fully developed. A set of performance data is summarized in **APPENDIX F**.

First a rough estimation of the size of the heat exchanger using overall heat transfer coefficients values, U from **TABLE 4.2**. From the table, the author has assumed for water to gas heat exchanger duty, the U value is $75 \text{ W/m}^2\cdot\text{K}$.

From the heat transfer equation, the author has used the heat transfer rate equation to find the heat transfer surface area, A .

$$\dot{Q} = UA\Delta T_{LM}$$

$$A = \frac{Q}{U\Delta T_{LM}}$$

$$A = \frac{306.128 \text{ kW}}{(75 \text{ W/m}^2\text{K})(18.13 \text{ K})} = 225.14 \text{ m}^2$$

Thus, the total heat transfer area surface required is 225.14 m^2 .

TABLE 4.2: Typical overall heat transfer coefficients

Heat Exchanger Duty	U (W/m ² .K)
Water-to-water	800-2000
Water-to-oil	100-350
Water-to-fuel	200-1000
Water-to-heat-transfer liquids	650-1500
Steam condenser	1000-6000
Refrigerant condenser	300-1000
Water-to-gas	40-75
Steam-to-gas	20-300
Gas-to-gas	10-40

4.5 Physical Characteristics of Fin Tube Heat Exchanger

For the fin tube heat exchanger, the copper tubes are arranged parallel to one another in staggered as illustrated in **FIGURE 4.1**. The chilled water is supplied through the tubes in the first row, circulated in the tube bank and leaving at the last row, while the ambient air entered the heat exchanger in cross flow direction with the chilled water in a cross flow method. Radial fins are used to enhance the heat transfer area are attached perpendicular to each of the tubes. Thus the primary surface area (outside area of bare copper tubes) is enhanced greatly by adding a secondary area of fins. The total area including fins is called total surface area, A_t for use in the calculations, in this report. The cross-section (Length x Height) across the heat exchanger which air flows is called the frontal area, A_{fi} .

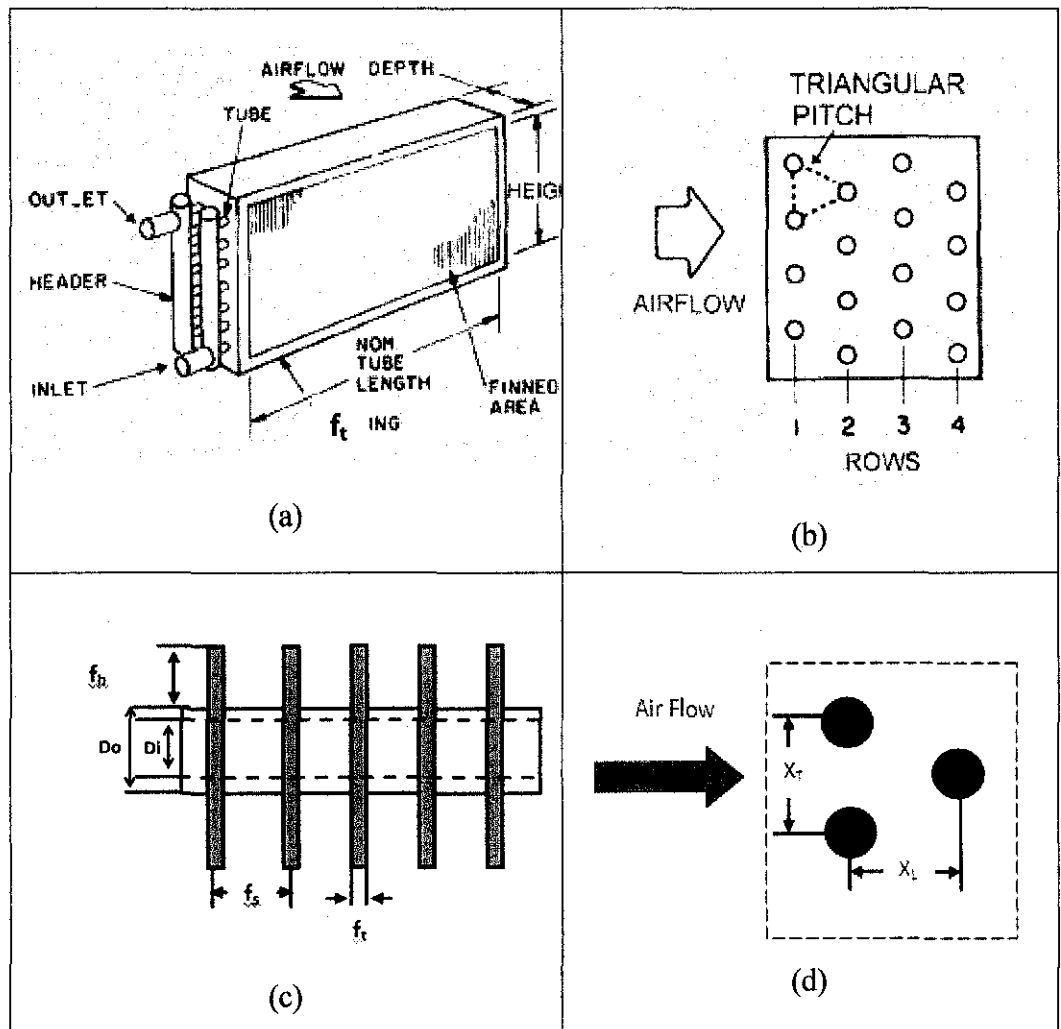


FIGURE 4.1: (a) Chilled water coil construction. (b) A 4-row coil with a 4-tube face. (c) Geometry of the radial fin perpendicular to tube. (d) Tube transverse and longitudinal pitch in tube bank

Thus, for this problem the author has figured out the initial estimation of the fin tube geometry. **TABLE 4.3** below shows the rough estimation of geometrical data for the fin tube heat exchanger taken from Sandar and Ulrich, (2003).

Table 4.3: The heat exchanger geometrical data

	Parameter	Value
Core	Length, L_1	1.25 m
	Depth, L_2	0.5 m
	Height, L_3	1.0 m
	No. of row, N_r	3
	No. of tube, N_t	18
	No. of fins/tube	143
	Transverse pitch, X_T	0.15 m
	Longitudinal pitch, X_L	0.15 m
Fin	Fin spacing, f_s	8.75×10^{-3} m
	Height, f_h	16.25×10^{-3} m
	Thickness, f_t	6.25×10^{-3} m
	Fin diameter, D_e	0.1075 m
	Material	Copper
Tube	Inside diameter, D_i	0.0675 m
	Outside diameter, D_o	0.0750 m
	Wall Thickness,	0.0075 m
	Material	Copper

4.6 Air Side

4.6.1 Reynolds Number, Re

The Reynolds number for cylinder form in cross-flow is based on the maximum velocity that occurs at the transverse plane. For staggered tube banks, the maximum velocity, U_{max} , can be defined as

$$U_{max} = \frac{X_T}{2(X_D - D_e)} U_{\infty}$$

Where u_{∞} , is the upstream velocity of air and can be found by the following equation,

$$u_{\infty} = \frac{\dot{m}_{air}}{A_{fr}\rho_{air}}$$

$$u_{\infty} = \frac{19 \text{ kg/s}}{(1.25 \text{ m}^2)(1.1614 \frac{\text{kg}}{\text{m}^3})} = 13.08 \text{ m/s}$$

and

$$X_D = \sqrt{X_L^2 + \left(\frac{X_T}{2}\right)^2}$$

$$X_D = \sqrt{(0.15)^2 + \left(\frac{0.15}{2}\right)^2} = 0.184 \text{ m}$$

Thus, the maximum velocity is

$$U_{max} = \frac{0.15}{2(0.184 - 0.1750)} (13.08) = 109 \text{ m/s}$$

For Reynolds number, which is, for a cylinder in cross flow is defined by this equation.

$$Re_D = \frac{U_{max}D}{\nu}$$

$$Re_D = \frac{\left(109 \frac{\text{m}}{\text{s}}\right)(0.0750 \text{ m})}{15.89 \times 10^{-6} \frac{\text{m}^2}{\text{s}}}$$

$$Re_D = 5.14 \times 10^5$$

Where,

ν = kinematic viscosity of air

D_o = outer diameter of tube

Thus, the flow is turbulent since, $Re_D > 2 \times 10^5$ and assumed to be steady flow and fully developed.

4.6.2 Convective Air Heat Transfer Coefficient

To calculate the heat transfer coefficient, first need to determine the Nusselt number, the author has used equation taken from Colburn, (1972), for heat transfer in cross flow air in staggered tube bank as follow,

$$Nu_D = 0.33Re_D^{0.6}Pr^{1/3}$$

$$Nu_D = 0.33(5.14 \times 10^5)^{0.6}(0.707)^{1/3}$$

$$Nu_D = 785.05$$

Thus, the heat-transfer coefficient for ambient air in the tube bank is

$$h = \frac{Nu_D k}{D_o}$$

$$h = \frac{(785.05) \left(0.0263 \frac{W}{m \cdot K}\right)}{0.0750 m} = 275.33 \frac{W}{m^2 \cdot K}$$

4.6.3 Pressure Loss

When ambient air flows across the tube bank, a pressure drop develops across the bank from the inlet to the outlet. The pressure drop can be calculated using the relations below taken from, *Kirk D. Hagen, Heat Transfer with Application, Prentice Hall, Inc. (1999)*.

$$\Delta p = N_L \Phi \frac{\rho U_{max}^2}{2} f$$

Where the friction factor, f , is determined using FIGURE and N_L is the number of rows in the tube bank. The correction factor, Φ , is applied when $X_T \neq X_L$. The values of f is depend on the Reynolds number, and parameter a and b . The

parameters a , b , can be defined as transverse and longitudinal pitch over outer diameter respectively.

$$a = \frac{X_T}{D} = \frac{0.25m}{0.075m} = 3.33$$

$$b = \frac{X_L}{D} = \frac{0.25m}{0.0750m} = 3.33$$

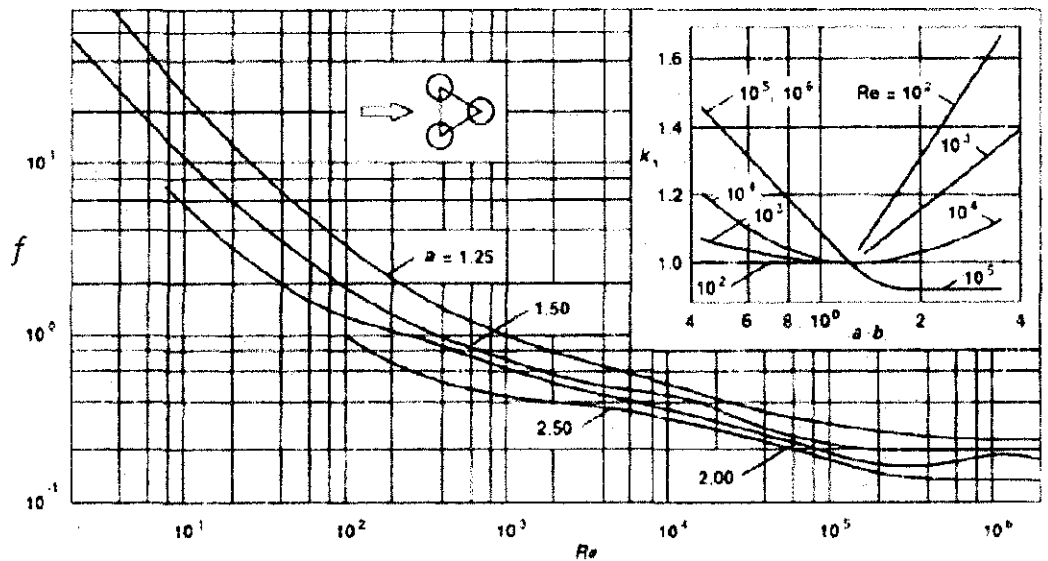


FIGURE 4.2: The friction factor for staggered tube bank is a function of the Reynolds number. (*Zhukanskas (1987)*)

From the **FIGURE 4.2**, the author estimated the friction factor to be, $f = 0.1$.

Since the $X_T = X_L$, correction factor, Φ , does not applied. Thus, the pressure loss in staggered tube bank can be defined by,

$$\Delta p = N_L \frac{\rho U_{max}^2}{2} f$$

$$\Delta p = (3) \left[\frac{(1.1614)(109)^2}{2} \right] (0.1)$$

$$\Delta p = 2.07 \text{ kPa}$$

4.7 Water Side

4.7.1 Reynolds Number, Re

First the author needed to compute the pipe flow area and velocity of the water using the following equation. Assumed that the tube is smooth surface and the flow is steady flow and fully developed and the area remains uniform along the tube.

$$\begin{aligned} \text{a) Pipe flow area: } A_i &= \frac{\pi}{4} D_i^2 \\ &= \frac{\pi}{4} (0.0675)^2 \\ &= 3.58 \times 10^{-3} \text{ m}^2 \end{aligned}$$

Mass velocity,

$$u_m = \frac{\dot{m}_2}{A_i \rho} = \frac{10.42 \text{ kg/s}}{(3.58 \times 10^{-3} \text{ m}^2)(1000 \text{ kg/m}^3)} = 2.91 \text{ m/s}$$

For internal flow in a circular pipe, the Reynolds number can be calculated from this equation where ν is the kinematic viscosity of the water and D_i is the inner diameter of tube,

$$Re = \frac{D_i u_m}{\nu} = \frac{(0.0675)(2.91)}{148.06 \times 10^{-8}} = 1.327 \times 10^5$$

4.7.2 Convective Water Heat Transfer Coefficient

Because the Reynolds number is greater than 10000, the flow is fully turbulent. In order to compute the value of Nusselt number and friction factor, the author used Gnielinski's correlation (1976), which can be applied if $1.00 < Pr < 10^5$ and $2300 < Re < 5 \times 10^6$. From the correlations, first need to find the friction factor, f

$$\begin{aligned} f &= \frac{1}{(1.82 \log_{10} Re - 1.64)^2} \\ &= \frac{1}{(1.82 \log_{10} 1.327 \times 10^5 - 1.64)^2} \end{aligned}$$

$$= \frac{1}{[1.82(5.123) - 1.64]^2}$$

$$= 0.0169$$

Then the correlation the author used to find the Nusselt number can be defined as below, with $f/8 = 0.0169/8 = 2.1 \times 10^{-3}$

$$Nu = \frac{\left(\frac{f}{8}\right)(Re - 1000)Pr}{1.00 + 12.7\left(\frac{f}{8}\right)^{\frac{1}{2}}(Pr^{\frac{2}{3}} - 1)}$$

$$= \frac{(2.1 \times 10^{-3})(1.327 \times 10^5 - 1000)(10.69)}{1.00 + 12.7(2.1 \times 10^{-3})^{\frac{1}{2}}[(10.69)^{\frac{2}{3}} - 1]}$$

$$= \frac{2.956 \times 10^3}{1.00 + (12.7)(0.0458)(4.853 - 1)}$$

$$= \frac{2.956 \times 10^3}{3.24}$$

$$= 912.03$$

Thus, the heat transfer coefficient of chilled water is,

$$h = \frac{k}{D_i} Nu = \frac{0.579}{0.0675} (912.03) = 7.823 \times 10^3 \frac{W}{m^2 \cdot K}$$

Where k , is thermal conductivity of the water and D_i is internal diameter of pipe.

4.7.3 Pressure Loss

Pressure drop in tubes can be estimated by first calculating the pressure drop for a straight tube in the bundles. Since the flow in the tubes is turbulent flow, the author used this Darcy-Weisbach correlation below to find pressure loss.

$$\Delta p = f \left(\frac{L}{D_h}\right) \left(\frac{\rho u_m^2}{2}\right)$$

Where;

f = Friction factor

L = Length of tube

D_h = Hydraulic diameter of tube

ρ = Water density

u_m = Water velocity in tube

Typical roughness values for several different pipe and ducts are given in **TABLE 4.4**. With roughness, ϵ for copper is $1.5 \times 10^{-6} \text{ m}$; the roughness ratio can be calculated:

$$\text{Roughness ratio} = D_t / \epsilon$$

$$= 0.0675 \text{ m} / 1.5 \times 10^{-6} \text{ m} = 45000$$

TABLE 4.4: Roughness for new pipe and ducts is a function of material and manufacturer. (Moody L.F, *Friction Factors for Pipe Flow* (1944)).

Pipe/Duct material	Roughness (mm)
Glass, plastic	0.0 (smooth)
Drawn tubing (copper, brass, etc.)	0.0015
Commercial steel and wrought iron	0.045
Cast iron, asphalt coated	0.12
Galvanized iron	0.15
Cast iron, uncoated	0.26
Concrete	0.3-3.0
Riveted steel	0.9-9.0
Fiberglass duct, rigid	0.9
Fiberglass duct liner, spray coated	3.0
Flexible duct, fabric and wire, fully extended	1.0-4.6
Flexible duct, metallic, fully extended	1.2-2.1

Knowing the Reynolds number and tube roughness, ε , enable the author to find the friction factor, f , using this equation. A mathematical formula that represents most of the transitional region and the entire turbulent of the Moody diagram has been given by Swamee and Jain, (1976) as below.

$$f = \frac{0.25}{\left[\log \left(\frac{1}{3.7 \left(\frac{D}{\varepsilon} \right)} + \frac{5.74}{Re_D^{0.9}} \right) \right]^2}$$

$$f = \frac{0.25}{\left[\log \left(\frac{1}{3.7(45000)} + \frac{5.74}{(1.327 \times 10^5)^{0.9}} \right) \right]^2} = 0.0170$$

Thus, the major loss for the single 1.25 m tube can be calculated with the Darcy-Weisbach Equation :

$$\begin{aligned} \Delta p &= f \left(\frac{L}{D_h} \right) \left(\frac{\rho u_m^2}{2} \right) \\ &= (0.0170) \left(\frac{1.25m}{0.0675m} \right) \left[\frac{(1000 \text{ kg/m}^3)(2.91\text{m/s})^2}{2} \right] \\ &= 0.916 \text{ kPa (for sigle tube)} \end{aligned}$$

So the total pressure loss in tube banks is the total pressure loss in all single tube.

$$\Delta p_T = \sum \Delta p, \text{ where number of tubes, } N = 18$$

$$\Delta p_T = 0.916 \text{ kPa} \times 18 = 16.488 \text{ kPa}$$

4.8 Overall Heat Transfer Coefficient

The overall heat transfer coefficient, U , can be defined as below. Here the author has neglected the wall and fouling thermal resistance.

$$U = \frac{1}{\frac{1}{h_w} + \frac{\Delta r}{k} + \frac{1}{h_a}}$$
$$= \frac{1}{\frac{1}{7.823 \times 10^3} + \frac{0.024}{52} + \frac{1}{275.33}}$$
$$U = 236.89 \frac{W}{m^2.K}$$

Where;

h_w = Heat transfer coefficient of water

h_a = Heat transfer coefficient of air

Δr = Outer radius of finned tube

k = Thermal conductivity of copper tube, 52 W/m.K

4.9 Fin Efficiency for Radial Fin

For this part, the author used the correlation based on Shah and Sekulic, (2003), that the performance of the fins is judged on the basis of enhancement of heat transfer relative to the no fin case. The performance of fins expressed in terms of the fin effectiveness, ε_{fn} . The overall effectiveness of the finned tube is

$$\varepsilon = \frac{\dot{Q}_{total\ fin}}{\dot{Q}_{total\ no\ fin}}$$

The first step is calculating the value of parameter m , where has units of inverse length and is defined by this equation below. Where k is thermal conductivity of the fin, t is the thickness of the fin and h_a is the heat transfer coefficient of ambient air. For this problem, the thermal conductivity of copper at 300 K is listed in **APPENDIX C** as $k = 52 \text{ W/m.K}$.

Parameter m ,

$$m = \sqrt{\frac{2h_a}{kt}}$$
$$m = \sqrt{\frac{2\left(275.33 \frac{W}{m^2 \cdot K}\right)}{\left(52 \frac{W}{m \cdot K}\right) (6.25 \times 10^{-3} m)}}$$
$$= 41.16 m^{-1}$$

The dimensionless quantities needed to obtain the fin efficiency from **FIGURE 2.5** are,

$$\phi = m(R_o - R_i)$$
$$= (41.16 m^{-1})(0.0538 - 0.0375)m = 0.67$$

And,

$$\frac{R_i}{R_o} = \frac{0.0375 m}{0.0538 m} = 0.69$$

Where;

R_i = tube radius from the center

R_o = radius of the fin from the center (fin tip)

(See **FIGURE 2.4**)

Hence the author estimated the fin efficiency, η , from the graph in **FIGURE 8** as,

$$\eta \approx 0.86$$

In the case of no fins, heat transfer from the tube per meter of its length is determined from Newton's law of cooling to be,

$$A_{no\ fin} = \pi D_o L = \pi(0.0750)(1.25) = 0.2945 m^2$$

$$\dot{Q}_{no\ fin} = h_a A_{no\ fin} (T_b - T_\infty)$$

$$= (275.33)(0.2945)(6 - 36) = -2.43 kW = 2.43 kW$$

Where T_b is the surface temperature and T_∞ is the fluid bulk temperature. And for the area and heat transfer rate of fin,

$$\begin{aligned}
 A_{fin} &= 2\pi(R_o^2 - R_i^2) + 2\pi R_i f_t \\
 &= 2\pi[(0.0538)^2 - (0.0375)^2] + 2\pi(0.0375)(6.25 \times 10^{-3}) \\
 &= 0.0108 \text{ m}^2
 \end{aligned}$$

$$\begin{aligned}
 \dot{Q}_{fin} &= \eta_{fin} h_a A_{fin} (T_b - T_\infty) \\
 &= (0.86)(275.33)(0.0108)(6 - 36) \\
 &= -0.077 \text{ kW} = 0.077 \text{ kW}
 \end{aligned}$$

Noting that the space between the two fins, S , is 8.75×10^{-3} m, heat transfer from the un-finned portion of the tube is

$$\begin{aligned}
 A_{unfin} &= \pi D_o S = \pi(0.0750)(8.75 \times 10^{-3}) \\
 &= 0.00206 \text{ m}^2
 \end{aligned}$$

$$\begin{aligned}
 \dot{Q}_{unfin} &= h A_{unfin} (T_b - T_\infty) \\
 &= (275.33)(0.00206)(6 - 36) \\
 &= -0.0017 \text{ kW} = 0.0017 \text{ kW}
 \end{aligned}$$

Thus, the total heat transfer from the finned tube becomes

$$\begin{aligned}
 \dot{Q}_{total \text{ fin}} &= N_f (\dot{Q}_{fin} + \dot{Q}_{unfin}) \\
 &= 143(0.077 + 0.0017) \text{ kW} = 11.25 \text{ kW}
 \end{aligned}$$

The overall effectiveness of the finned tube is

$$\varepsilon = \frac{\dot{Q}_{total \text{ fin}}}{\dot{Q}_{total \text{ no fin}}} = \frac{11.25 \text{ kW}}{2.43 \text{ kW}} = 4.63$$

4.10 Heat Transfer Area

In this part, the author has computed the heat transfer area of the heat exchanger based on the fin geometry explained earlier. The total heat transfer area A_t consist of the area associated with the exposed tubes and header plates (primary surface area), A_p , and the fins (secondary surface area), A_f . Where δ is the fin thickness, N_f is the number of fins per unit length, and N_t is the number of tubes, Ramesh K. Shah and P. Sekulic, (2003).

$$A_p = \pi D_o (L_1 - \delta N_f L_1) N_t + 2(L_2 L_3 - \frac{\pi D_o^2}{4} N_t)$$

$$\begin{aligned} A_p &= \pi(0.0750)[(1.25 - (6.25 \times 10^{-3})(143)(1.25)](18) + \\ &2 \left[(0.5)(1.0) - \frac{\pi(0.0750)^2}{4} (18) \right] \\ &= 1.404 \text{ m}^2 \end{aligned}$$

$$\begin{aligned} A_f &= \left[\frac{2\pi(D_e^2 - D_o^2)}{4} + \pi D_e \delta \right] N_f L_1 N_t \\ &= \left[\frac{2\pi[(0.1075^2 - 0.0750^2)]}{4} + \pi(0.0750)(6.25 \times 10^{-3}) \right] (143)(1.25)(18) \\ &= 34.7 \text{ m}^2 \end{aligned}$$

Hence, the total surface area is the sum of the primary and secondary surface area.

$$\begin{aligned} A_t &= A_p + A_f \\ &= 1.404 + 34.7 \\ &= 36.104 \text{ m}^2 \end{aligned}$$

The minimum free-flow area for the tube arrangement is that area for a tube bank minus the area blocked by the fins:

$$A_o = \left[(X_t - D_o)L_1 - (D_e - D_o)\delta N_f L_1 \right] \frac{L_3}{X_t}$$

$$\begin{aligned} &= [(0.15 - 0.075)(1.25) - (0.1075 - 0.075)(6.25 \times 10^{-3})(79)(1.25)] \frac{1.0}{0.15} \\ &= 0.49 \text{ m}^2 \end{aligned}$$

Frontal area surface;

$$\begin{aligned} A_{fr} &= L_1 L_3 \\ &= (1)(1.25) \\ &= 1.25 \text{ m}^2 \end{aligned}$$

CHAPTER 5

RESULTS & DISCUSSION

5.1 General

In order to perform the heat transfer analysis of an exchanger design, the important variables of the author best interest are the tube size diameter, number of rows and fin spacing. The six samples data are extrapolated in the spreadsheet as in **APPENDIX F** for comparison the best design heat exchanger. The analysis is concentrated on getting variable of air exit temperature, heat transfer rate, water mass flow rate, flow characteristic, total heat transfer area surface and. A new design model of heat exchanger is essential to acquire the largest temperature reduction, higher overall heat transfer coefficient, higher heat transfer rate and smaller pressure drop.

5.2 The Effect of Ambient Temperature on the Chilled Water Mass Flow Rate

In general, for increasing inlet temperature the chilled water mass flow rate will be increased because of increasing heat load in order to control the air leaving the heat exchanger (20°C) prior of entering the gas turbine inlet. The ambient air temperature effect on the chilled water mass flow rate is shown in **FIGURE 5.1**. Theoretically, the heat transfer rate is increased as the ambient temperature increase in order to have the desired maximum temperature reduction of air outlet as shown in **FIGURE 5.2**.

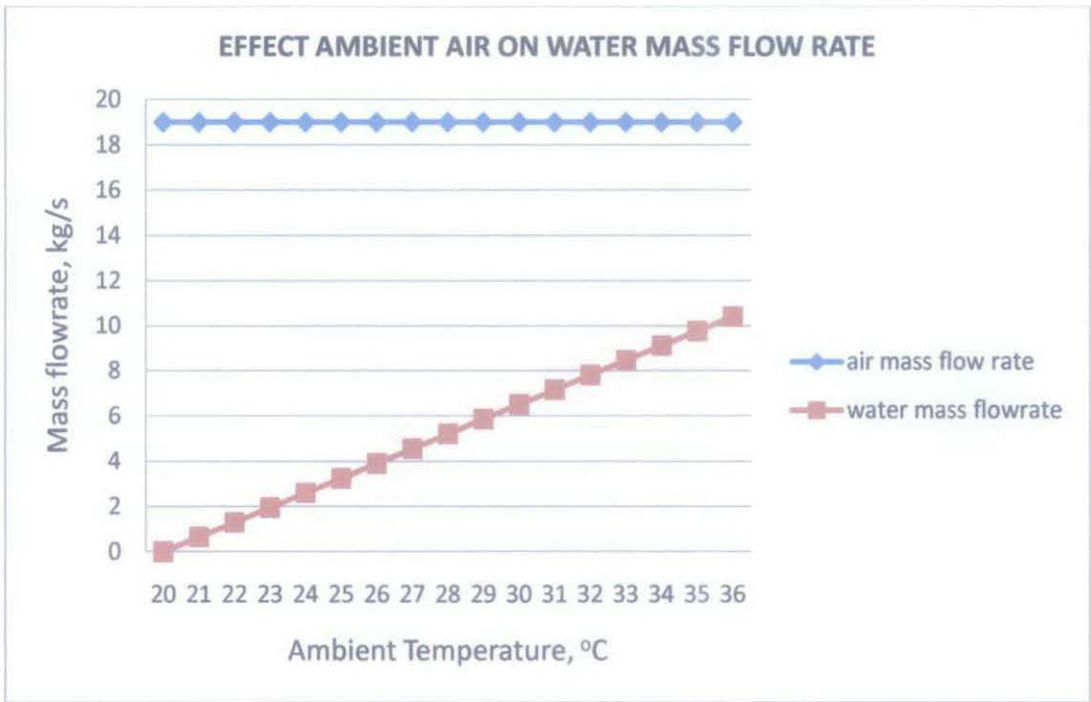


FIGURE 5.1: Ambient air temperature vs. mass flow rate

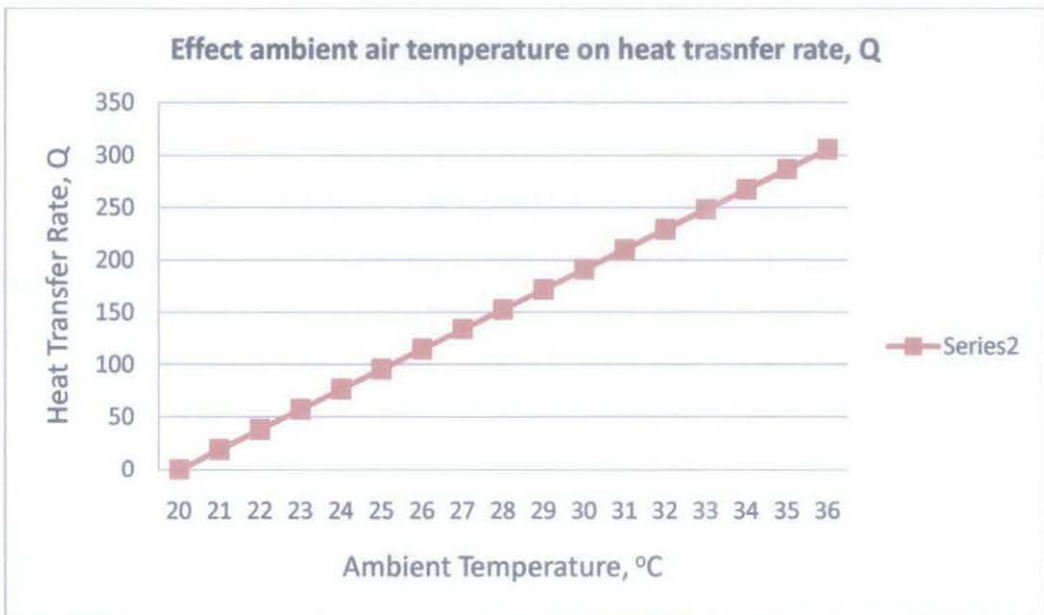


FIGURE 5.2: Ambient air temperature vs Heat transfer rate

5.3 Analytical Model Results for Heat Exchanger Design

The analytical model results of the heat exchanger design, including heat transfer rate, heat transfer coefficient for air side, and overall heat transfer coefficient for each row of the heat exchanger, pressure drop and heat exchanger effectiveness are shown in the **APPENDIX G**. Air leaving temperature and water mass flow rate entering the heat exchanger which must be controlled according to the requirements of present study. The author has presented these values in the graph for comparison. Below are the variables output that the author are concentrating.

5.3.1 Effect of Number of Row to the Total Heat Transfer Rate for Air Side

The total heat transfer rate for air side, it is the summed of the heat transfer rate in fin and tubes as shown mention earlier in the Chapter 4. The heat transfer rate is depending on the surface area of contact between the fluids which is in this case is gas-to-fluid. The increasing in tube diameter meaning the addition of the surface area for the cross flow air thus, increasing the heat transfer rate. Adding the rows is another option for increasing the heat transfer rate which is in the case of fixed frontal area. As shown in the **FIGURE 5.3**. From the Chapter 4, the required heat transfer rate to maintain the outlet temperature (20 °C) is 306.128 kW. Thus, the author used it as the reference point in order to find the best design.



FIGURE 5.3: Total heat transfer rate vs number of rows

5.3.2 Effect of Tube Diameter to the Heat Transfer Coefficient

As been mention earlier in the Literature Review, the staggered tube arrangement for the air cooled heat exchanger is chose instead of the in-line tube bank because of the high heat transfer rate. We assume that the frontal area of the heat exchanger fixed and the air mass flow rate is constant through the heat exchanger. Thus, from the graph in the **FIGURE 5.4** the author had to conclude that the increasing size of tube diameter has caused the heat transfer coefficient of the system is increased directly. This is because the minimal area flow of the air, A_o is reduced and thus the flow restriction has increased.

For the internal pipe, the heat transfer rate in decreasing as the tube diameter in increasing as shown in the **FIGURE 5.5**. Theoretically, the heat transfer rate in the internal pipe is depending on the fluid velocity which is the chilled water. Increasing the tube diameter has made the area inlet of the pipe is bigger thus the water velocity became smaller as been described in the Chapter 4 in this report. Thus, for the final design, the author has to consider the tube diameter which is most suitable for the problem and has the highest value of heat transfer coefficient for both fluids.

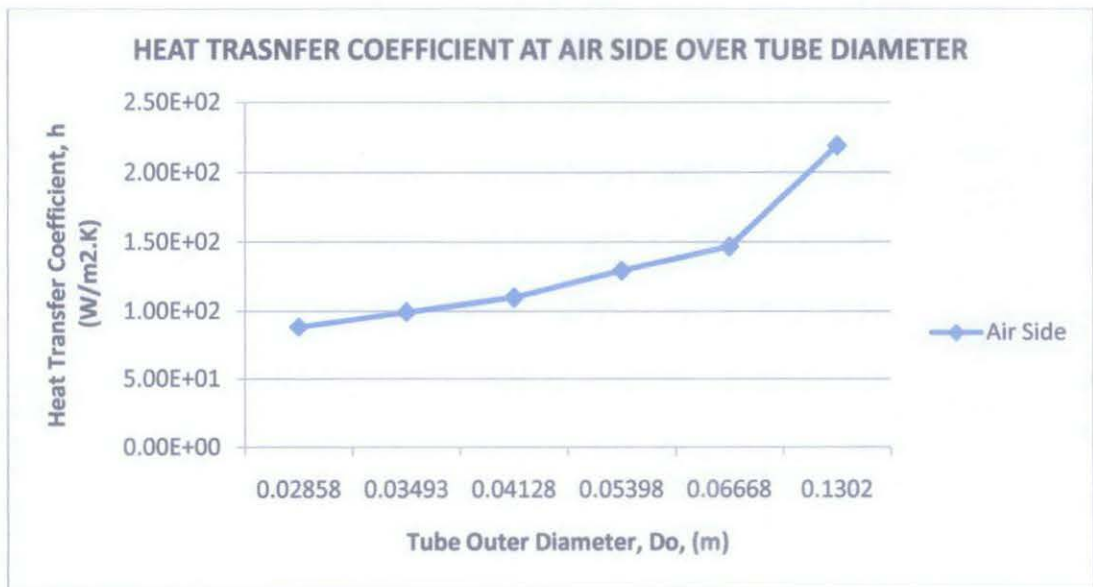


FIGURE 5.4: Heat Transfer Coefficient Vs Tube Diameter for Air Side

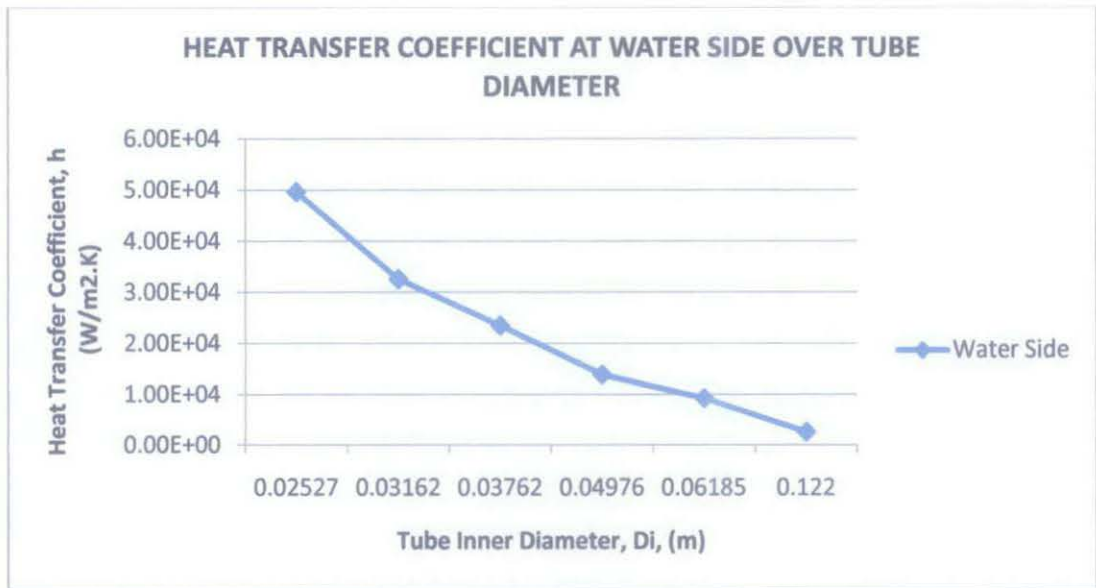


FIGURE 5.5: Heat Transfer Coefficient Vs Tube Diameter for Water Side

5.3.3 Effect of Number of Rows to the Pressure Drop

From the literature review, the author had assumed that the staggered tube bank has greater heat transfer rate, also has higher pressure drop. The staggered arrangement of the tube has caused the flow of air is restricted and thus slowing down the speed and at the same time pressure is dropped. The increasing the number of rows has continuously increased the pressure drop of air as shown in **FIGURE 5.6**.

For the water side, the pressure drop is also increased as shown in the **FIGURE 5.7**. The pressure drop in the inner pipe is smaller compare to the air side, yet it is to avoid the minimal as it could. The pressure drop for the inner pipe is based on the summed of the pressure drop in single pipe. Thus, when the tubes number is increased the total pressure also increased. These all six sample has different values of pressure drop, which the author has to figure out which design has the allowable pressure drop.

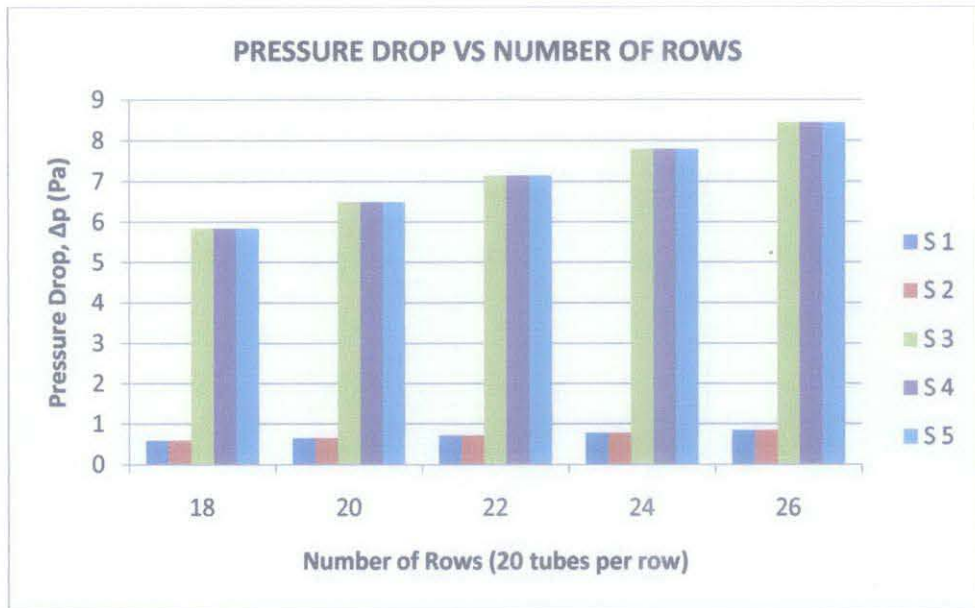


FIGURE 5.6: Pressure drop vs number of rows for air side

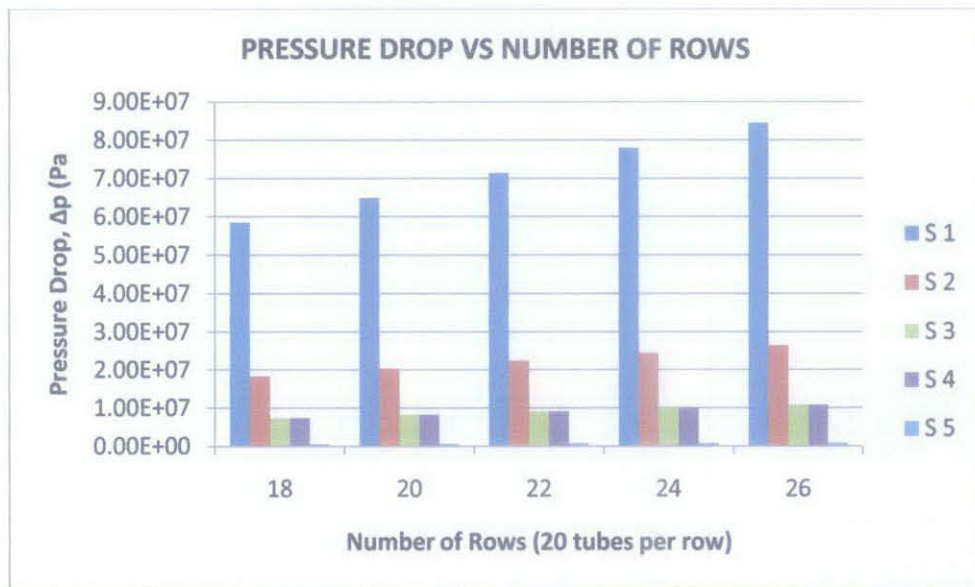


FIGURE 5.7: Pressure drop vs number of rows for water side

5.3.4 The Air Outlet Temperature

The outlet temperature of air, T_o can be determined by using energy balance and is given by this equation below (Khan, et al. 2006), where N_T is the number of tubes in any given row, N is the total number of tubes in the bank, h , U_∞ , and X_T is the air heat transfer coefficient, mass velocity and transverse pitch respectively. The author has used this

equation since the outlet temperature is known, to find the total number of tubes and tube diameter of the design.

$$T_w - T_o = (T_w - T_i) \exp\left(\frac{-\pi D_o N h}{\rho U_\infty N_T X_T C_p}\right)$$

$$T_o = T_w - (T_w - T_i) \exp\left(\frac{-\pi D_o N h}{\rho U_\infty N_T X_T C_p}\right)$$

The result is shown in the **FIGURE 5.8**. For this problem, the required air outlet temperature is 20 °C , thus the sample has the value laid within the region is to be considered. Based on the graph in **FIGURE 5.8**, sample 5 and sample 6 is the only that meet the requirement and narrowed down the number of options. In the end the author has to determine which one is the most optimum design of the fin tube heat exchanger.

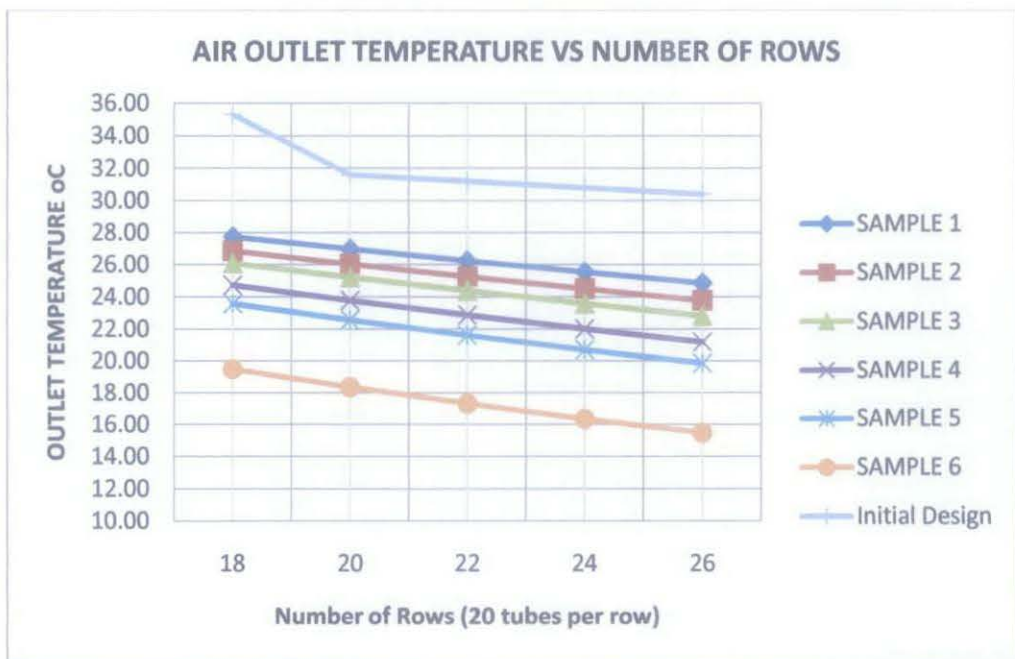


FIGURE 5.8: Air outlet temperature comparison for the samples based on the number of row in the tube bank

5.4 Final Core Design

From the initial design, the author has assumed the fin geometry and characteristics are fixed. The only variables that have been looking into are the number of rows (number of tubes) and the tube diameter. Thus, for this section, the author has concluded the design of the fin tube heat exchanger based on the analysis earlier. The design parameters are summarized in the **TABLE 5.1** below.

TABLE 5.1: Final design of the fin tube heat exchanger

	Parameter	Value
Core	Length, L_1	1.75 m
	Depth, L_2	1.0 m
	Height, L_3	1.25 m
	No. of row, N_r	26
	No. of tube, N_t	520
	No. of fins/tube	1094
	Transverse pitch, X_T	0.25 m
	Longitudinal pitch, X_L	0.25 m
Fin	Fin spacing, f_s	8.75×10^{-3} m
	Height, f_h	16.25×10^{-3} m
	Thickness, f_t	6.25×10^{-3} m
	Fin diameter, D_e	0.1075 m
	Material	Copper
Tube	Inside diameter, D_i	0.06185 m
	Outside diameter, D_o	0.06668 m
	Wall Thickness,	0.00483 m
	Material	Copper

Below is the general geometry of the fin tube heat exchanger developed in the 3D model using the CATIA software (**FIGURE 5.9**). The design consisted 26 rows of horizontal tube pipe arranged in staggered manner, parallel to each other.

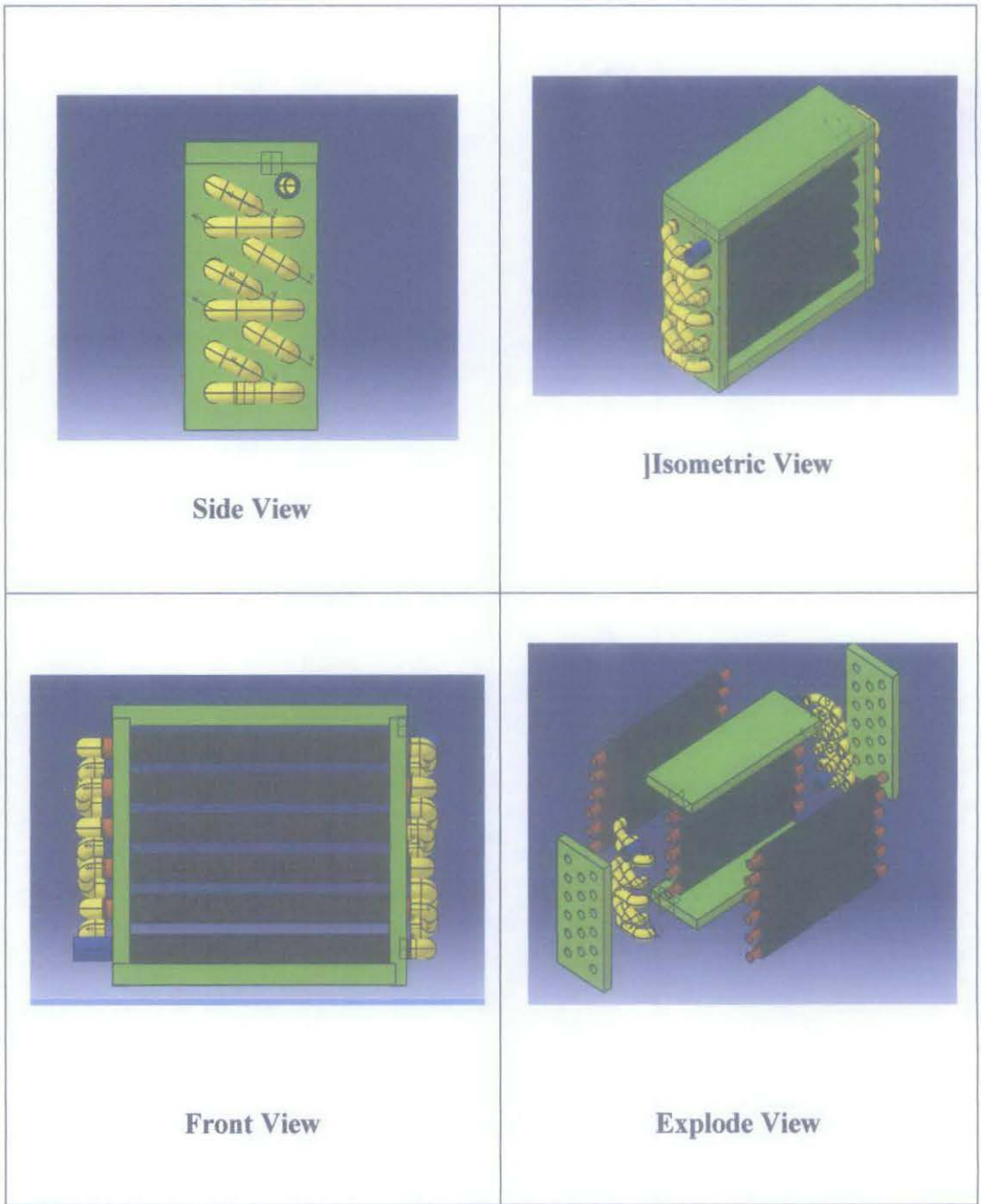


FIGURE 5.9: General configuration of fin tube heat exchanger.

CHAPTER 6

CONCLUSION

Nevertheless, taking into account all the design innovations, the actual performances of the equipment are still heavily penalized by the ambient intake air temperature, particularly in tropical humid and hot dry zones. There are various methods which are commercially available for turbine air inlet cooling aiming to improve gas turbine efficiency. In this project a same approach has been proposed by the author to improve gas turbines performance. The idea is to cool inlet air of the gas turbines by heat exchanger using chilled water. The design is developed based on the operating parameter of the GTE and absorption chiller in the GDC. Several samples have successfully been analyzed by the author to have the desired outlet temperature and heat transfer rate. The radial fin attached at the tube has able to enhance the heat transfer coefficient of the system. The final design of the fin tube heat exchanger is presented in 3D model. As the conclusion, apart from this result, the author has fulfilled the objectives of the project and completed the Final Year Project 2.

CHAPTER 7

RECOMMENDATIONS

For the recommendations, the author has listed out some improvements on the methods and experimental works in order to have more precise data and design model. For further analysis, the fin geometry and characteristic should be taken into consideration during the designing and validation phase. Study has shown that fin spacing and thickness as well as the type of fin to be used in the heat exchanger have a major role in the heat transfer coefficients and pressure drop. Second is, the fluid flow analysis using Computational Fluid Dynamics (CFD) software, has to be made to have more promising results from the variables mentioned in this report. Lastly, the system should be improved more in terms of the design and the method used in order to be placed at the inlet of the gas turbine engine.

6. REFERENCES

- A. A. Amell, Francisco J. Cadavid, 2002, *Influence of the relative humidity on the air cooling thermal load in gas turbine power plant* [Journal]. Gas Science and Technology Group, Faculty of Engineering, University of Antioquia, Calle 67 No. 53-108 Bloque 20-435, Medellin, Colombia, Applied Thermal Engineering, 1529-1533.
- A. P. Colburn, 1933, *A method of correlating forced convection heat transfer data and a comparison with fluid friction*, Trans,Inst Chem. Eng. 29, p.174-210.
- A. Zhukasukas, 1987, *Convective Heat Transfer in Cross Flow*.
- K. D. Hagen, 1999, *Heat Transfer with Applications*, Prentice Hall International, Inc. Weber State University
- P. K., Swamee and A. K. Jain, 1976, *Ecplicit Equations for Pipe-Flow Problems*, J. Hydraulics Div. 102 (HY5): 657-664. New York: American society of Civil Engineers.
- R. K. Shah and Dušan P. Sekulic, 2003, *Fundamentals of Heat Exchanger Design.*, Rochester Institute of Technology, Rochester, New York
- S. B. Genic, Brainslav M. Jacimovic, Boris R. Latinovic, 2006, *Research on air pressure drop in helically-finned tube heat exchangers* [Journal], Department of Process Engineering, Faculty of Mechanical Engineering, University of Belgrade, Kraljice Marije 16, 11000 Beograd, Serbia and Montenegro, Applied Thermal Engineering, 26 478-485.
- UTP Gas District Cooling Plant, *Operational Manual and Gas Turbine Engine*
- W.A. Khan, J.R. Culham, M.M. Yovanovich, 2006, *Convection heat transfer from tube banks in crossflow: Analytical approach* [Journal]. Department of Mathematics, CIIT Abbottabad, NWFP, 22060 Pakistan, International Journal of Heat and Mass transfer, 4831-4838

APPENDIX A: THERMAL PROPERTIES OF SATURATED LIQUID WATER

(H₂O)

Table E-1 Thermal properties of saturated liquid water (H₂O) *

<i>T</i> (K)	ρ (kg/m ³)	<i>C_p</i> (J/kg-K)	$\mu \times 10^7$ (kg/m-s)	$\nu \times 10^8$ (m ² /s)	<i>k</i> × 10 ³ (W/m-K)	$\alpha \times 10^6$ (m ² /s)	<i>Pr</i>	$\beta \times 10^4$ (K ⁻¹)
273	999.8	4.217	17.525	175.3	569	13.50	12.90	6.010
283	999.7	4.193	12.992	129.9	586	13.98	9.30	10.00
293	998.7	4.182	10.015	100.3	602	14.42	6.96	2.41
303	995.7	4.179	7.970	80.04	617	14.83	5.40	2.00
313	992.3	4.179	6.513	65.64	630	15.19	4.32	3.01
323	988.0	4.181	5.440	55.06	643	15.57	3.54	4.15
333	983.2	4.185	4.630	47.09	653	15.87	2.97	4.00
343	977.7	4.190	4.095	40.96	662	16.16	2.54	5.40
353	971.6	4.197	3.510	36.13	669	16.44	2.20	6.17
363	965.2	4.205	3.113	31.25	675	16.63	1.94	6.00
373	958.1	4.216	2.790	29.12	680	16.83	1.73	7.00
383	950.7	4.229	2.522	26.53	683	16.99	1.56	8.00
393	942.9	4.245	2.300	24.39	685	17.11	1.43	8.77
403	934.6	4.263	2.110	22.58	687	17.24	1.31	9.17
413	925.8	4.283	1.930	21.00	687	17.32	1.22	9.93
423	916.8	4.310	1.810	19.74	686	17.36	1.14	1.040
433	907.3	4.339	1.690	18.63	684	17.37	1.07	1.100
443	897.3	4.371	1.585	17.66	681	17.36	1.02	1.158
453	886.9	4.408	1.493	16.83	676	17.29	0.974	1.200
463	876.0	4.449	1.412	16.12	671	17.22	0.936	1.200
473	864.7	4.497	1.338	15.47	664	17.08	0.906	1.220
483	840.3	4.514	1.245	14.46	648	16.71	0.865	1.400
513	813.6	4.770	1.114	13.69	629	16.21	0.845	1.600
533	783.9	4.985	1.030	13.14	604	15.46	0.850	1.944
553	750.5	5.300	961	12.81	573	14.41	0.830	2.300
573	712.2	5.770	901	12.63	540	13.14	0.963	3.000
593	666.9	6.500	830	12.45	503	11.43	1.09	3.900
613	610.1	8.270	768	12.26	460	9.117	1.34	5.400
633	528.0	14.990	644	12.19	401	5.064	2.41	8.010

*From [8].

APPENDIX B: THERMAL PROPERTIES OF GASES AT ATMOSPHERIC PRESSURE

Table B-1 Thermal properties of gases at atmospheric pressure.*

T (K)	ρ (kg/m ³)	c_p (J/kg·K)	$\mu \times 10^7$ (kg/m·s)	$\nu \times 10^6$ (m ² /s)	$k \times 10^3$ (W/m·K)	$\alpha \times 10^6$ (m ² /s)	Pr
Air							
100	1.2922	1.005	171.1	2.00	9.34	2.54	0.786
150	1.2464	1.012	183.4	4.426	13.8	5.64	0.758
200	1.2048	1.007	192.5	7.590	18.1	10.3	0.737
250	1.1667	1.006	199.6	11.44	22.3	15.9	0.720
300	1.1314	1.007	184.6	15.89	26.3	22.5	0.707
350	0.9950	1.009	208.2	20.92	30.0	29.9	0.700
400	0.8711	1.014	230.1	26.41	33.8	38.3	0.690
450	0.7740	1.021	250.7	32.39	37.3	47.2	0.686
500	0.6964	1.030	270.1	38.79	40.7	56.7	0.684
550	0.6329	1.040	288.4	45.57	43.9	66.7	0.685
600	0.5804	1.051	305.8	52.69	46.9	76.9	0.685
650	0.5356	1.063	322.5	60.21	49.7	87.3	0.690
700	0.4975	1.075	338.8	68.10	52.4	98.0	0.695
750	0.4643	1.087	354.6	76.37	54.9	109	0.702
800	0.4354	1.099	369.8	84.93	57.3	120	0.709
850	0.4097	1.110	384.3	93.80	59.6	131	0.716
900	0.3868	1.121	398.1	102.9	62.0	143	0.720
950	0.3666	1.131	411.3	112.2	64.3	155	0.723
1,000	0.3482	1.141	424.4	121.9	66.7	168	0.726
1,100	0.3166	1.159	449.0	141.8	71.5	195	0.728
1,200	0.2902	1.175	471.0	162.9	76.3	224	0.728
1,300	0.2679	1.190	496.0	185.1	82	238	0.720
1,400	0.2488	1.207	527	212	91	303	0.699
1,500	0.2322	1.230	557	240	100	350	0.685
1,600	0.2177	1.248	584	268	106	390	0.688
1,700	0.2049	1.267	611	298	113	435	0.685
1,800	0.1938	1.286	637	329	120	482	0.683
1,900	0.1833	1.307	663	362	128	534	0.677
2,000	0.1741	1.337	689	396	137	589	0.672
2,100	0.1658	1.372	715	431	147	646	0.667
2,200	0.1582	1.417	740	468	160	714	0.655
2,300	0.1513	1.478	766	506	175	783	0.647
2,400	0.1448	1.558	792	547	196	869	0.630
2,500	0.1389	1.665	818	589	222	960	0.613

APPENDIX C: THERMAL PROPERTIES OF METALLIC SOLIDS

READING THERMAL PROPERTIES

Thermal properties in this and subsequent appendices are read as follows: The thermal diffusivity of pure aluminum, for example, is read as $\alpha \times 10^5 = 9.71$. Hence, $\alpha = 9.71 \times 10^{-5} \text{ m}^2/\text{s}$.

Table C-1 Thermal properties of metallic solids at 300 K*

Metal	T_{melt} (K)	ρ (kg/m ³)	c_p (J/kg·K)	k (W/m·K)	$\alpha \times 10^5$ (m ² /s)
Aluminum					
Pure	933	2,702	903	237	9.71
1060 temp	935	2,770	875	174	7.18
Alloy 105, cast	883	2,790	883	168	6.82
1300	925	2,713	921	222	8.88
2024	775	2,770	875	177	7.30
3003	922	2,790	921	192	7.61
5052	894	2,685	921	138	5.58
6061	880	2,713	903	180	6.89
6063	907	2,713	962	218	8.34
7075	830	2,796	963	121	4.49
Argonium	1,350	1,820	1,820	200	5.92
Bismuth	545	9,780	122	7.86	0.659
Cadmium	594	8,650	231	96.8	1.81
Copper					
Pure	1,356	8,933	385	401	11.7
99.99%	1,356	8,961	385	391	11.4
ETP	1,347	8,913	385	388	11.3
Red brass	1,280	8,714	385	61	1.82
Yellow brass	1,190	8,470	377	116	3.63
Bronzes, commercial	1,297	8,830	377	52	1.56
Constantan, 40% Ni	1,333	8,920	410	22.7	0.621
Wire, drawn		8,900	385	287	8.38

APPENDIX D: PIPE DIMENSIONS

Table D-1 Type K copper tubing.

Nominal Size (in.)	Inside Diameter (mm)	Outside Diameter (mm)	Wall Thickness (mm)	Flow Area (m ²)
3/8	4.572	6.35	0.889	1.642×10^{-5}
1/2	7.036	9.53	1.245	3.888×10^{-5}
3/4	11.31	12.70	1.245	8.180×10^{-5}
1	13.39	15.88	1.245	1.407×10^{-4}
1 1/8	16.56	19.05	1.245	2.154×10^{-4}
1 1/2	18.92	22.23	1.651	2.812×10^{-4}
1 3/4	25.27	28.58	1.651	5.017×10^{-4}
2	31.62	34.93	1.651	7.854×10^{-4}
2 1/2	37.62	41.28	1.829	1.111×10^{-3}
3	49.76	53.98	2.108	1.948×10^{-3}
3 1/2	61.85	66.68	2.413	3.004×10^{-3}
4	73.84	79.38	2.769	4.282×10^{-3}
4 1/2	85.98	92.08	3.048	5.806×10^{-3}
5	97.97	104.8	3.404	7.538×10^{-3}
6	122.0	130.2	4.061	1.170×10^{-2}
8	145.8	155.6	4.877	1.670×10^{-2}
10	192.6	206.4	6.883	2.914×10^{-2}
12	240.0	257.2	8.585	4.524×10^{-2}
14	287.4	308.0	10.287	6.487×10^{-2}

APPENDIX F: HEAT EXCHANGER PERFORMANCE SPREADSHEET

							WATER SIDE			
Do	Di	Reynolds Number	Nusselt number	Heat Transfer Coefficients, h (W/m ² .K)	Pressure Drop, ΔP (Pa)	Reynolds Number	Nusselt number	Heat Transfer Coefficients, h (W/m ² .K)	Pressure Drop, ΔP (Pa)	
Nr = 18, Tube = 360										
S 1	0.02858	0.02527	18831.72	107.9579	99.34545049	1.14585	354616	2166.649	49643.4368	116100.6
S 2	0.03493	0.03162	23015.82	121.7689	91.68397604	1.14585	283401.2	1779.552	32585.73194	36357.44
S 3	0.04128	0.03762	27199.91	134.6049	85.75846478	11.4585	238201.7	1528.124	23518.9752	14791.61
S 4	0.05398	0.04976	35568.11	158.1091	77.0335161	11.4585	180087.3	1196.303	13920.00164	3481.198
S 5	0.06668	0.06185	43936.3	179.4793	70.79044409	11.4585	144885.1	989.2021	9260.274666	1130.996
S 6	0.1302	0.122	85790.43	268.1537	54.16621379	458.3401	73452.02	546.8793	2595.435269	33.90751
Nr = 20, Tube = 400										
S 1	0.02858	0.02527	18831.72	107.9579	99.34545049	1.273167	354616	2166.649	49643.4368	116100.6
S 2	0.03493	0.03162	23015.82	121.7689	91.68397604	1.273167	283401.2	1779.552	32585.73194	36357.44
S 3	0.04128	0.03762	27199.91	134.6049	85.75846478	12.73167	238201.7	1528.124	23518.9752	14791.61
S 4	0.05398	0.04976	35568.11	158.1091	77.0335161	12.73167	180087.3	1196.303	13920.00164	3481.198
S 5	0.06668	0.06185	43936.3	179.4793	70.79044409	12.73167	144885.1	989.2021	9260.274666	1130.996
S 6	0.1302	0.122	85790.43	268.1537	54.16621379	509.2667	73452.02	546.8793	2595.435269	33.90751

APPENDIX F: (CONTINUED)

						WATER SIDE				
Do (m)	Di (m)	Reynolds Number	Nusselt number	Heat Transfer Coefficients, h (W/m ² .K)	Pressure Drop, ΔP (Pa)	Reynolds Number	Nusselt number	Heat Transfer Coefficients, h (W/m ² .K)	Pressure Drop, ΔP (Pa)	
Nr = 24, Tube = 480										
S 1	0.02858	0.02527	18831.72	107.9579	99.34545049	1.5278	354616	2166.649	49643.4368	116100.6
S 2	0.03493	0.03162	23015.82	121.7689	91.68397604	1.5278	283401.2	1779.552	32585.73194	36357.44
S 3	0.04128	0.03762	27199.91	134.6049	85.75846478	15.278	238201.7	1528.124	23518.9752	14791.61
S 4	0.05398	0.04976	35568.11	158.1091	77.0335161	15.278	180087.3	1196.303	13920.00164	3481.198
S 5	0.06668	0.06185	43936.3	179.4793	70.79044409	15.278	144885.1	989.2021	9260.274666	1130.996
S 6	0.1302	0.122	85790.43	268.1537	54.16621379	611.1201	73452.02	546.8793	2595.435269	33.90751
Nr = 26, Tube = 520										
S 1	0.02858	0.02527	18831.72	107.9579	99.34545049	1.655117	354616	2166.649	49643.4368	116100.6
S 2	0.03493	0.03162	23015.82	121.7689	91.68397604	1.655117	283401.2	1779.552	32585.73194	36357.44
S 3	0.04128	0.03762	27199.91	134.6049	85.75846478	16.55117	238201.7	1528.124	23518.9752	14791.61
S 4	0.05398	0.04976	35568.11	158.1091	77.0335161	16.55117	180087.3	1196.303	13920.00164	3481.198
S 5	0.06668	0.06185	43936.3	179.4793	70.79044409	16.55117	144885.1	989.2021	9260.274666	1130.996
S 6	0.1302	0.122	85790.43	268.1537	54.16621379	662.0468	73452.02	546.8793	2595.435269	33.90751

APPENDIX G: THE OVERALL PERFORMANCE OF HEAT EXCHANGER SPREADSHEET.

	Do (m)	Di (m)	Fin Effectiveness, ϵ	Total Surface Area, m ²	Overall Heat Transfer Coefficients, U, (W/m ² .K)	Outlet Temperature, T _o (°C)	Total Heat Transfer Rate, Q (W)
	Nr = 18, Tube = 360						
S 1	0.02858	0.02527	6.8185007	340.4072	97.60061	27.75458	604631
S 2	0.03493	0.03162	6.667431291	404.5618	90.11016	26.87832	662353.4
S 3	0.04128	0.03762	6.562839147	468.6708	84.24803	26.09559	717408.2
S 4	0.05398	0.04976	6.42747777	596.752	75.58288	24.73761	819535.3
S 5	0.06668	0.06185	6.343678764	724.6507	69.33261	23.58272	912906.6
S 6	0.1302	0.122	6.169911674	1361.608	52.35374	19.50349	1295390
	Nr = 20, Tube = 400						
S 1	0.02858	0.02527	6.8185007	377.9525	97.60061	26.99147	671067.3
S 2	0.03493	0.03162	6.667431291	449.2353	90.11016	26.05413	735215.7
S 3	0.04128	0.03762	6.562839147	520.4676	84.24803	25.22053	796392.5
S 4	0.05398	0.04976	6.42747777	662.78	75.58288	23.78288	909864.9
S 5	0.06668	0.06185	6.343678764	804.8897	69.33261	22.56931	1013600
S 6	0.1302	0.122	6.169911674	1512.62	52.35374	18.35738	1438489
	Nr = 22, Tube = 440						
S 1	0.02858	0.02527	6.8185007	415.4977	97.60061	26.25513	737503.6
S 2	0.03493	0.03162	6.667431291	493.9089	90.11016	25.26248	808077.9
S 3	0.04128	0.03762	6.562839147	572.2643	84.24803	24.38356	875376.8
S 4	0.05398	0.04976	6.42747777	728.808	75.58288	22.87681	1000195
S 5	0.06668	0.06185	6.343678764	885.1286	69.33261	21.61431	1114294
S 6	0.1302	0.122	6.169911674	1663.632	52.35374	17.30855	1581589

APPENDIX G: (CONTINUED)

	Do (m)	Di (m)	Fin Effectiveness, ϵ	Total Surface Area, m (m ²)	Overall Heat Transfer Coefficients, U, (W/m ² .K)	Outlet Temperature, T _o (°C)	Total Heat Transfer Rate, Q (W)
	Nr = 24, Tube = 480						
S 1	0.02858	0.02527	6.8185007	453.043	97.60061	25.54462	803939.8
S 2	0.03493	0.03162	6.667431291	538.5824	90.11016	24.50207	880940.2
S 3	0.04128	0.03762	6.562839147	624.0611	84.24803	23.58304	954361.1
S 4	0.05398	0.04976	6.42747777	794.8359	75.58288	22.0169	1090524
S 5	0.06668	0.06185	6.343678764	965.3676	69.33261	20.71435	1214987
S 6	0.1302	0.122	6.169911674	1814.644	52.35374	16.34874	1724688
	Nr = 26, Tube = 520						
S 1	0.02858	0.02527	6.8185007	490.5882	97.60061	24.85903	870376.1
S 2	0.03493	0.03162	6.667431291	583.2559	90.11016	23.77169	953802.5
S 3	0.04128	0.03762	6.562839147	675.8578	84.24803	22.81738	1033345
S 4	0.05398	0.04976	6.42747777	860.8639	75.58288	21.2008	1180854
S 5	0.06668	0.06185	6.343678764	1045.607	69.33261	19.86626	1315681
S 6	0.1302	0.122	6.169911674	1965.656	52.35374	15.47039	1867787